

1 **Title:** Interpretation of temporal and spatial trends of SARS-CoV-2 RNA in San Francisco Bay  
2 Area wastewater  
3

4 **Author names and affiliations:**

5 Hannah D. Greenwald<sup>a,b\*</sup> and Lauren C. Kennedy<sup>a,b\*</sup>, Adrian Hinkle<sup>a,b</sup>, Oscar N. Whitney<sup>c</sup>,  
6 Vinson B. Fan<sup>c</sup>, Alexander Crits-Christoph<sup>d,e</sup>, Sasha Harris-Lovett<sup>b</sup>, Avi I. Flamholz<sup>c,f</sup>, Basem Al-  
7 Shayeb<sup>d,e</sup>, Lauren D. Liao<sup>g</sup>, Matt Beyers<sup>h</sup>, Daniel Brown<sup>i</sup>, Alicia R. Chakrabarti<sup>j</sup>, Jason Dow<sup>k</sup>,  
8 Dan Frost<sup>l</sup>, Mark Koekemoer<sup>k</sup>, Chris Lynch<sup>i</sup>, Payal Sarkar<sup>m</sup>, Eileen White<sup>j</sup>, Rose Kantor<sup>a,b</sup>, Kara  
9 L. Nelson<sup>a,b,e</sup>

10

11 \*Authors contributed equally to the work

12 a: Department of Civil and Environmental Engineering, University of California, Berkeley, CA, USA

13 b: Berkeley Water Center, University of California, Berkeley, CA, USA

14 c: Department of Molecular and Cell Biology, University of California, Berkeley, CA, USA

15 d: Department of Plant and Microbial Biology, University of California, Berkeley, CA, USA

16 e: Innovative Genomics Institute, Berkeley, CA, USA

17 f: Division of Biology and Biological Engineering, California Institute of Technology, Pasadena, CA, USA

18 g: School of Public Health, University of California, Berkeley, CA, USA

19 h: Alameda County Public Health Department, San Leandro, CA, USA

20 i: Contra Costa Health Services, Martinez, CA, USA

21 j: East Bay Municipal Utility District, Oakland, CA, USA

22 k: Central Marin Sanitation Agency, San Rafael, CA, USA

23 l: Central Contra Costa Sanitary District, Martinez, CA, USA

24 m: San José-Santa Clara Regional Wastewater Facility, San José, CA, USA

25 See Supplementary Information for author contributions.

26

27 **Corresponding authors:**

28 Rose Kantor, [rkantor@berkeley.edu](mailto:rkantor@berkeley.edu)

29 Kara L. Nelson, [karanelson@berkeley.edu](mailto:karanelson@berkeley.edu)

30

31

32

33

34

35

36

37

38

39

40

41

42

43

44

45

46

## ABSTRACT

47 Wastewater surveillance for severe acute respiratory syndrome coronavirus 2 (SARS-CoV-2)  
48 RNA can be integrated with COVID-19 case data to inform timely pandemic response. However,  
49 more research is needed to apply and develop systematic methods to interpret the true SARS-  
50 CoV-2 signal from noise introduced in wastewater samples (e.g., from sewer conditions, sampling  
51 and extraction methods, etc.). In this study, raw wastewater was collected weekly from five  
52 sewersheds and one residential facility, and wastewater SARS-CoV-2 concentrations were  
53 compared to geocoded COVID-19 clinical testing data. SARS-CoV-2 was reliably detected (95%  
54 positivity) in frozen wastewater samples when reported daily new COVID-19 cases were 2.4 or  
55 more per 100,000 people. To adjust for variation in sample fecal content, crAssphage, pepper  
56 mild mottle virus, *Bacteroides* ribosomal RNA (rRNA), and human 18S rRNA were evaluated as  
57 normalization biomarkers, and crAssphage displayed the least spatial and temporal variability.  
58 Both unnormalized SARS-CoV-2 RNA signal and signal normalized to crAssphage had positive  
59 and significant correlation with clinical testing data (Kendall's Tau-b ( $\tau$ )=0.43 and 0.38,  
60 respectively). Locational dependencies and the date associated with testing data impacted the  
61 lead time of wastewater for clinical trends, and no lead time was observed when the sample  
62 collection date (versus the result date) was used for both wastewater and clinical testing data.  
63 This study supports that trends in wastewater surveillance data reflect trends in COVID-19  
64 disease occurrence and presents approaches that could be applied to make wastewater signal  
65 more interpretable and comparable across studies.

66

67 **Keywords:** COVID-19, wastewater-based epidemiology, pepper mild mottle virus, crAssphage,  
68 *Bacteroides*, human 18S rRNA

## 69 1. INTRODUCTION

70 Increasing hospitalizations and limited diagnostic testing capacity early in the coronavirus disease  
71 2019 (COVID-19) pandemic made it clear that multiple methods to monitor circulation of severe  
72 acute respiratory syndrome coronavirus 2 (SARS-CoV-2) are needed (Bivins et al., 2020). One  
73 such method is wastewater-based epidemiology (WBE), which has provided community-scale  
74 information on drug use, personal care products, antibiotic resistance, and pathogen circulation  
75 (Choi et al., 2018). SARS-CoV-2 is a promising candidate for WBE because its RNA is detected  
76 in stool of infected individuals (Li et al., 2021; Parasa et al., 2020), and wastewater surveillance  
77 has been shown to provide early detection of population-level increases in occurrence compared  
78 to clinical data in some locations (Ahmed et al., 2021; D'Aoust et al., 2021a; Gerrity et al., 2021;  
79 Hata and Honda, 2020; Medema et al., 2020; Nemudryi et al., 2020; Peccia et al., 2020; Randazzo  
80 et al., 2020b, 2020a).

81  
82 Together, wastewater and clinical testing might provide more reliable information about disease  
83 burden in communities than either method alone. Clinical testing of individuals is resource-  
84 intensive and has well-known biases (e.g., selection bias based on symptom severity, symptom  
85 recognition, occupation, etc.) (Catalogue of Bias Collaboration et al., 2017; Griffith et al., 2020;  
86 Sims and Kasprzyk-Hordern, 2020), which have compounded negative impacts in communities  
87 with higher proportions of low-income residents and of Black, Indigenous, and People of Color,  
88 including in the San Francisco Bay Area (Chamie et al., 2020; Misa et al., 2020). In contrast, WBE  
89 may provide a less biased assessment of COVID-19 occurrence (Murakami et al., 2020; Sims  
90 and Kasprzyk-Hordern, 2020). For COVID-19 WBE to be useful for public health decision-making,  
91 a better understanding is needed of the variability of SARS-CoV-2 in wastewater and how it  
92 relates to the true incidence or prevalence of COVID-19 in the contributing population (McClary-  
93 Gutierrez et al., 2021). Sources of target signal variability in wastewater include inconsistencies  
94 in sample collection and laboratory processing (Ahmed et al., 2020d; Feng et al., 2021), nucleic

95 acid degradation based on travel time and conditions in the sewer (Hart and Halden, 2020a), and  
96 signal dilution due to rainfall and diurnal flow changes (Zahedi et al., 2021). Researchers have  
97 addressed some of these sources of variability through normalization to biomarkers, increased  
98 sampling frequency, processing biological replicates, and smoothing/forecasting (D'Aoust et al.,  
99 2021b; Feng et al., 2021; Graham et al., 2020; McLellan et al., 2021; Nemudryi et al., 2020;  
100 Stadler et al., 2020).

101  
102 Normalization of target signal to flow, population, and/or an endogenous biomarker has the  
103 potential to reduce variability and scale values for comparisons across samples and locations.  
104 Across WBE studies, researchers have normalized wastewater concentrations to flow rate and  
105 population to calculate a per capita load (Chen et al., 2014; Choi et al., 2018; Zuccato et al., 2005;  
106 Zuccato Ettore et al., 2008) or to a chemical parameter (e.g., caffeine) (Been et al., 2014; Choi et  
107 al., 2018; D'Aoust et al., 2021b; Polo et al., 2020). More recently, four biological markers have  
108 emerged as promising candidates to normalize SARS-CoV-2 RNA signal for fecal content. Pepper  
109 mild mottle virus (PMMoV), a nonenveloped RNA plant virus, is commonly used for COVID-19  
110 WBE (D'Aoust et al., 2021b; Feng et al., 2021; Whitney et al., 2021; Wu et al., 2020) but  
111 concentrations in sewage vary with season and local diet (Symonds et al., 2019). Another  
112 normalization biomarker is the cross-assembly phage (crAssphage), a non-enveloped, DNA virus  
113 that ubiquitously infects the human gut commensal bacteria *Bacteroides* (Edwards et al., 2019;  
114 Green et al., 2020; Stachler et al., 2017; Wilder et al., 2021). In addition, *Bacteroides* HF183 16S  
115 rRNA gene is widely used for detecting fecal contamination in environmental waters (Green et al.,  
116 2020; Shanks et al., 2008), and recent studies (D'Aoust et al., 2021b; Kapoor et al., 2015;  
117 Pitkänen et al., 2013) have targeted HF183 rRNA (versus the rRNA gene) to increase the  
118 sensitivity of the assay (D'Aoust et al., 2021b; Feng et al., 2021). Lastly, the human 18S ribosomal  
119 subunit RNA (18S rRNA) assay has been proposed as a normalization biomarker because it  
120 targets human cells that are shed in feces (D'Aoust et al., 2021b; Whitney et al., 2021). While

121 each of these normalization biomarkers has been assessed independently, they have not all been  
122 compared within the same study.

123  
124 In addition to normalizing the target signal, smoothing procedures can assist in discerning  
125 temporal trends in SARS-CoV-2 occurrence. While seven-day moving averages have been widely  
126 used for assessing clinical data trends in real-time (“Track Testing Trends,” n.d.), wastewater  
127 sampling is often performed only 1-3 times per week. Therefore, smoothing techniques are  
128 needed that can be applied to data with lower sampling frequency that minimize loss of temporal  
129 resolution, such as locally weighted scatterplot smoothing (Lowess) (Gibas et al., 2021; Gonzalez  
130 et al., 2020; Nemudryi et al., 2020; Vallejo et al., 2020). However, no standard value for the  
131 bandwidth parameter exists (analogous to the selection of a seven-day window for moving  
132 averages of clinical data), and the default parameter value differs between two common  
133 languages used for data analysis (R (“Source code for spatialEco package,” n.d.): 0.75 and  
134 Python (“Source code for statsmodels module,” n.d.): 0.67). Furthermore, the bandwidth selection  
135 process generally has not been specified in studies incorporating Lowess (Gibas et al., 2021;  
136 Gonzalez et al., 2020; Nemudryi et al., 2020; Vallejo et al., 2020; Wu et al., 2020).

137  
138 Systematic approaches are also needed to estimate the minimum number of clinical COVID-19  
139 cases for which SARS-CoV-2 RNA is reliably detected in wastewater (WBE case detection limit).  
140 The WBE case detection limit is dependent on the methods used to extract genetic material as  
141 well as the extent of local clinical testing and may require sewershed-specific assessment.  
142 However, a systematic approach to estimate this value across studies can aid interpretation of  
143 nondetects and elucidate the number of COVID-19 cases per capita above which COVID-19 WBE  
144 will be a reliable public health surveillance strategy. In a recent study (Wu et al., 2021), a WBE  
145 case detection limit was estimated using a dataset with 1,687 samples, which was large enough  
146 to include repeated wastewater measurements at low case numbers. With fewer data points,

147 researchers have estimated this value observationally by reporting the number of cases they were  
148 able to detect or quantify (Hata and Honda, 2020; Medema et al., 2020).

149  
150 The goal of this research was to develop and assess approaches for COVID-19 WBE data  
151 validation and interpretation. Specific objectives were to: (i) evaluate normalization biomarkers  
152 (crAssphage, pepper mild mottle virus, Bacteroides rRNA, and human 18S rRNA) for adjusting  
153 SARS-CoV-2 RNA signal to account for variable wastewater fecal content; (ii) assess SARS-  
154 CoV-2 wastewater testing as a complement to clinical testing for public health surveillance by  
155 determining the correlation between these two methods; (iii) determine whether wastewater  
156 trends lead clinical trends and could provide early warning of COVID-19 outbreaks; (iv) evaluate  
157 a systematic method for trendline smoothing; (v) develop a systematic method for estimating a  
158 WBE case detection limit; and (vi) apply these methods to interpret spatial and temporal trends  
159 in COVID-19 occurrence based on wastewater and clinical testing data. We analyzed a sample  
160 set from six locations in the San Francisco Bay Area containing 5 months of weekly raw  
161 wastewater samples paired with geocoded clinical data.

162

## 163 **2. MATERIALS AND METHODS**

164 Six locations in the San Francisco Bay area were sampled (referred to throughout as locations A,  
165 S, N, K, Q, and E). Raw wastewater was collected weekly and archived from April to September  
166 2020, and biological replicates were processed for some locations as indicated in **Table 1**. SARS-  
167 CoV-2 and normalization biomarkers (crAssphage, PMMoV, Bacteroides rRNA, and 18S rRNA)  
168 were measured in wastewater samples via RT-qPCR. Associated physicochemical data were  
169 collected by wastewater utilities, and associated geocoded clinical COVID-19 data were collected  
170 by public health departments (Table 1).

171

172

## 173 **2.1 Wastewater sample collection and physicochemical data**

174 24-hour time-weighted composite samples of raw wastewater were collected using Teledyne  
175 ISCO autosamplers. Some samples were collected and processed in biological replicate (i.e.,  
176 wastewater subsamples were aliquoted from the same composite sample but independently  
177 extracted). After collection, all samples were transported to the lab on ice, stored at either -20°C  
178 or -80°C, and then thawed at 4°C for 36-48 hours before extractions. Wastewater data was not  
179 individually identifiable; therefore, no IRB was needed. More information on location-specific data  
180 collection and wastewater sampling, transport, storage, and biological replicates is provided in  
181 **Table 1** and the **Supplementary Information (SI) Section A**.

182  
183 One rainfall event occurred (May 12-19) during which sampling locations experienced 0.8 to 1.8  
184 inches of precipitation ([NOAA Climate Data Online database](#)). Although none of the sampled  
185 locations was a combined sewer system, rainfall could still increase flow rates through infiltration  
186 and inflow. Daily wastewater flow rate values during this period varied <4% (Locations K & E,  
187 **Table S1**), which is negligible when compared to the variation displayed by normalization  
188 biomarkers over time (15%-244%; **Figure 1**). Mean flow rates were provided by the wastewater  
189 utility for locations A, N, and S and were calculated from daily flow rates for locations K, E, and Q  
190 (**Table 1** and **SI Section A**).

## 191 192 **2.2 Clinical testing and population data**

193 Geospatial vector data of the sewersheds (locations S, K, A, and N) were used to determine the  
194 COVID-19 clinical testing data that mapped to each wastewater catchment area (**Table 1**). For all  
195 locations, daily new case data correspond to the date that results were reported (result date) for  
196 each COVID-19 test. For location K, additional data were available that correspond to the sample  
197 collection date and the episode date, defined as the earliest of: (i) the date of first symptoms; (ii)  
198 the sample collection date; or (iii) the date the sample was received by the testing lab. Clinical

199 testing data were provided by the corresponding county or open data portal (**Table 1**). Data were  
200 masked by public health departments to maintain confidentiality of the contributing population  
201 (below 11 new cases per day) and were provided as 7-day (A, S, K) or 14-day (N) moving  
202 averages. Masked values were substituted at 5.5 new cases per day for further analysis and  
203 plotting. For San Quentin Prison (location Q), unmasked COVID-19 clinical data were obtained  
204 from the California Department of Corrections and Rehabilitation open data portal (“CDCR  
205 Population COVID-19 Tracking,” n.d.), and instances of zero cases were substituted at 0.5 cases  
206 for comparison to masked data in statistical data analysis (**Figure 5**). For clinical data obtained  
207 for this study, no IRB was needed because data were either provided masked or were publicly  
208 available. More information about masking and population data is provided in **Table 1** and **SI**  
209 **Section E**.

210

### 211 **2.3 Wastewater sample processing via the 4S method**

212 Wastewater samples were concentrated and extracted following the 4S method (Whitney, 2020;  
213 Whitney et al., 2021), with a minor modification: the elution buffer was not pre-warmed; instead,  
214 it was added to the column, and the column was heated at 50°C for 10 minutes before  
215 centrifugation to collect the eluate. Both RNA and DNA were captured (**Figure S1**). Each  
216 extraction batch contained a negative extraction control, and each sample or control was spiked  
217 with a surrogate virus control (Bovilis coronavirus; Merck Animal Health, BCoV) and a free RNA  
218 control (synthetic oligomer construct, SOC). Because it is not possible to independently quantify  
219 the surrogate spike without the influence of extraction efficiency (Kantor et al., 2021), extraction  
220 controls were used to assess consistency of extractions rather than recovery. Outlier analysis  
221 ( $\alpha=0.05$ ) was conducted for BCoV and SOC Cq values using Grubbs test. No outliers were  
222 detected, and all samples tested were considered to have passed this quality control screen.  
223 Wastewater sample processing is further described in **SI Section B**.

224



## 225 2.4 RT-qPCR plate setup, controls, and data processing

226 Reverse transcription quantitative polymerase chain reaction (RT-qPCR) was performed on  
227 wastewater extract targeting eight sequences: (i) SARS-CoV-2 CDC nucleocapsid gene (N1)  
228 assay duplexed with (ii) VetMAX™ Xeno™ Internal Positive Control (Xeno) assay, (iii)  
229 crAssphage CPQ\_056 (crAssphage) assay, (iv) pepper mild mottle virus coat protein gene  
230 (PMMoV) assay, (v) *Bacteroides* 16S ribosomal RNA HF183/BacR287 (*Bacteroides* rRNA) assay,  
231 (vi) bovine coronavirus transmembrane protein gene (BCoV) assay, (vii) Synthetic Oligomer  
232 Construct T33-21 free-RNA (SOC) assay, and (viii) human 18S ribosomal subunit RNA (18S  
233 rRNA) assay (Greenwald, 2021). Reaction conditions (**Table S2**), thermocycling conditions  
234 (**Table S3**), and primers, amplicon sequences, and probes (**Table S4**) are included in the SI.  
235 Reactions consisted of 20  $\mu$ L total volume, including 5  $\mu$ L of RNA extract, TaqMan Fast Virus 1-  
236 Step Master Mix (ThermoFisher Scientific), primers, probes, and nuclease-free water. Reactions  
237 were completed on a QuantStudio 3 Real-Time qPCR system (ThermoFisher Scientific), where  
238 Cq values were determined through automatic thresholding on QuantStudio 3 Design and  
239 Analysis Software (v1.5.1). Every plate included samples, no-template controls (NTCs), and  
240 standards, each quantified in technical triplicate (qPCR replicates). Individual standard curves  
241 (efficiencies ranging from 83.2% to 97.8% and  $R^2$  ranging from 0.974 to 0.999 for the N1 standard  
242 (Twist Bioscience)) were used as a quality control measure (**Table S5**) and later combined into  
243 master standard curves (**Table S6**) to calculate quantities (Ahmed et al., 2020c, 2021). A subset  
244 of samples were run with no reverse transcription (no-RT) controls for *Bacteroides* rRNA and 18S  
245 rRNA, and RNA was found to be multiple orders of magnitude greater than DNA in the samples  
246 tested (**Table S7**). Further details on RT-qPCR materials and no-RT controls are provided in the  
247 **SI Section C**.

248

249 Raw Cq values that did not amplify or that amplified below the limit of detection were substituted  
250 with the Cq value corresponding to half the limit of detection (for N1) or half the lowest point of

251 the master standard curve (for all other assays) (**Table S6**), and then outliers were assessed  
252 using a two-sided Grubbs test ( $\alpha=0.05$ ). The N1 qPCR limit of detection (LoD) was calculated  
253 by analyzing all RNA standard curves from the study as well as four additional extended triplicate  
254 standard curves. The N1 LoD was set at 5 gene copies per reaction, at which point 67% of  
255 technical replicates were positive (**Table S8**). Further details on the data processing pipeline are  
256 provided in **SI Section D**.

257

## 258 **2.5 Assessing PCR inhibition via serial dilution and an internal amplification control**

259 To our knowledge, there is no standard methodology for assessing PCR inhibition in raw  
260 wastewater samples. We combined two approaches to assess PCR inhibition in raw wastewater  
261 samples: a non-competitive internal amplification control (Ahmed et al., 2020b; Nolan et al., 2006;  
262 Schrader et al., 2012; Staley et al., 2012) and serial dilution (Graham et al., 2020). The internal  
263 amplification control can easily be included in every sample, but cannot detect assay-specific  
264 inhibition (Schrader et al., 2012). Serial dilution consumes more resources and risks diluting the  
265 target signal below the detection limit, but it more accurately tests the target itself and allows  
266 selection of a dilution value that best reduces the impacts of inhibition. Thus, we used the  
267 VetMAX™ Xeno™ Internal Positive Control (ThermoFisher Scientific) as a screening tool to select  
268 samples for further testing with serial dilution.

269

270 For all samples, Xeno RNA was spiked into the reaction mix (**Table S2**), and NTCs were used as  
271 an inhibition-free baseline to compare each sample on that plate. Ten samples showed  $>2$  Cq  
272 deviation from the baseline and were selected for further inhibition testing (Staley et al., 2012). A  
273 dilution series (1x, 2x, 5x, 10x) was performed on these samples, and the duplexed N1 and Xeno  
274 assay was repeated. A dilution was chosen by comparing SARS-CoV-2 N1 signal in each dilution  
275 to theoretical expectations (based on theoretical doubling per PCR cycle). If diluting the sample  
276 led to a 1 Cq difference between actual and expected change in Cq, then the sample at the base

277 dilution was deemed inhibited (Graham et al., 2020). Following the serial dilution test, only three  
278 samples required dilution (**Table S9**), and subsequent qPCR results in this study are reported  
279 using this chosen dilution. Results from the internal amplification control were inconsistent with  
280 inhibition assessed via serial dilution, and we do not recommend the use of Xeno for testing N1  
281 inhibition in future studies.

282

## 283 **2.6 Data analysis**

284 All data analysis was performed in Python (v3.6.9) using key modules Pandas (v1.1.5), NumPy  
285 (v1.19.5), SciPy (v1.4.1), and Plotnine (v0.6.0).

286

### 287 2.6.1 Normalization biomarker analyses

288 For N1 normalization to biomarkers, N1 (gene copies per liter, gc/L) was divided by the  
289 normalization biomarker concentration (gc/L). To calculate flow-scaled biomarker load  
290 (gc/person/day), target concentration (gc/L) was multiplied by mean flow for the sampling location  
291 (MGD) and a unit conversion factor (liter per million gallons) and then divided by population. Daily  
292 flow rate data were not available for S, N, and A (locations upstream of a treatment facility) (**Table**  
293 **S1**), so mean dry weather flow rates (and population) were used to scale data when comparing  
294 across locations. We expect that the mean flow rate likely approximates the daily flow rate  
295 throughout the study period, but this may not hold true in different locations and seasons.

296

297 For comparisons of biomarker concentrations and variation (**Figure 1**), a Kruskal-Wallis test  
298 (SciPy v1.4.1) was performed, followed by pairwise Dunn's tests (scikit-posthocs v0.6.6) to  
299 determine statistical differences. Rank correlations between wastewater and case data (**Figure**  
300 **2**) were calculated as Kendall's Tau-b coefficients ( $\tau$ ; SciPy v1.4.1), a method adapted for left-  
301 censored data (i.e., datasets with data below a lower limit of detection) (Wood et al., 2011)  
302 because 22% of the data are below the N1 LoD. Correlations were classified as low ( $\tau < 0.3$ ),

303 moderate ( $0.3 < \tau < 0.5$ ), or high ( $\tau > 0.5$ ). Coefficients of variation (CV) were calculated as the  
304 arithmetic standard deviation divided by the mean, while geometric coefficient of variation (gCV)  
305 was calculated as the geometric standard deviation minus one.

306

### 307 2.6.2 Assessment of WBE case detection limit

308 The WBE case detection limit was estimated as follows. The paired wastewater and case data  
309 for all sewersheds were combined and sorted from highest to lowest case counts. For each case  
310 count, all technical replicates in the wastewater data at and above that point were tallied to  
311 determine the cumulative percentage of replicates that amplified in RT-qPCR. Equation 1 was  
312 used to fit a logistic function (Kyurkchiev and Markov, 2016) to the dataset (SciPy v1.4.1), where  
313  $y$  is the fraction of amplified technical replicates,  $x$  is the  $\log_{10}$ (moving average of new cases per  
314 person per day),  $k$  sets the growth rate of  $y$ , and  $\gamma$  sets the inflection point. Zero new cases per  
315 capita cannot be represented in a logistic growth model, but in this study, case values of zero  
316 were only available for location Q, and these values were substituted as 0.5 cases before the  
317 analysis. The COVID-19 per capita case rate that corresponded to 95% cumulative amplification  
318 of technical replicates was reported as the estimated WBE case detection limit, and the analysis  
319 was repeated with samples where daily per capita cases were provided as masked values.

320

$$321 \quad y = \frac{1}{1+e^{(-k*(x-\gamma))}} \text{ (Equation 1)}$$

322

### 323 2.6.3 Wastewater trendline smoothing

324 For wastewater data, any smoothed trendline displayed in a figure was determined using a fitted  
325 local regression (Lowess; statsmodels v0.10.2) with bandwidth parameter ( $\alpha$ , the fraction of the  
326 dataset used for smoothing), set as previously shown (Jacoby, 2000) (**Figures 3 and S2-S5**).  
327 Lowess trends of SARS-CoV-2 N1 signal were also visualized as heatmaps to aid in discerning

328 peaks (**Figures S6 and S7**). Full dataset and associated code are available through GitHub  
329 (<https://zenodo.org/record/4730990#.YlxrqlKgUo>).

330

### 331 **3. RESULTS**

332 Raw wastewater was collected weekly from April to September 2020 at six locations (**Table 1**).

333 The resulting dataset includes 91 samples (155 including biological replicates), analyzed for

334 SARS-CoV-2 and four potential normalization biomarkers (crAssphage, PMMoV, *Bacteroides*

335 rRNA, and human 18S rRNA) and paired with geocoded clinical testing data. This dataset was

336 generated from the San Francisco Bay Area in separate sanitary sewer systems during a period

337 with minimal rainfall (see Methods), which naturally controlled for variability in wastewater strength

338 due to precipitation. Thus, we expected the concentrations of the measured normalization

339 biomarkers to be relatively stable. Additionally, geocoded clinical testing data included a range of

340 per capita COVID-19 case rates that varied by location.

341

#### 342 **3.1 CrAssphage and PMMoV were the most consistent biomarkers**

343 A subset of samples from all locations were used in experiments (**Figure 1**) comparing

344 crAssphage (98 unique samples, 153 biological replicates), PMMoV (93 unique samples, 95

345 biological replicates), *Bacteroides* rRNA (97 unique samples, 99 biological replicates) and 18S

346 rRNA (40 unique samples, 41 biological replicates) as biomarkers for normalization to fecal

347 content. All normalization biomarkers were detected at high concentrations (**Table S10**) in all

348 samples tested, except for 18S rRNA, which was inconsistently quantifiable (**Figure S8**). Flow

349 rates and chemical wastewater parameters (TSS, BOD, COD, cBOD) were not consistently

350 measured by utilities (**Table S1**); thus, robust comparisons of physicochemical biomarkers could

351 not be made. In the absence of daily flow rate data, we used mean flow rate to scale wastewater

352 biomarker concentrations by per capita wastewater flow for each sewershed to account for

353 differences across sewersheds (**Figure 1**). Mean per capita flow rates were similar for all locations

354 except Q (a facility; **Table 1**), generally resulting in little change after flow-scaling. For this reason,  
355 flow-scaling was applied to compare biomarkers, but unnormalized SARS-CoV-2 N1  
356 concentrations are used as a baseline in later analyses.

357  
358 An ideal normalization biomarker would have minimal spatial variation in per capita shedding rates  
359 and minimal temporal differences in wastewater loads when flow rates are stable, as they were  
360 in this study. Two methods were used to evaluate biomarker variability (**Figure 1**): (i) comparing  
361 per capita biomarker loads (gene copies/person/day) to assess differences in observed shedding  
362 by location; and (ii) evaluating the temporal variation of loads for each location. Consistent with  
363 recent studies (Ahmed et al., 2020d; D'Aoust et al., 2021b), crAssphage and PMMoV were the  
364 least variable biomarkers across locations and over time (mean  $gCV_{crAssphage}=59\%$  and mean  
365  $gCV_{PMMoV}=56\%$ , not statistically different ( $p>0.05$ )). In contrast, *Bacteroides* rRNA displayed more  
366 variability both spatially (**Figure 1**) and temporally (mean  $gCV=130\%$ ), and 18S rRNA varied  
367 dramatically (mean  $gCV=500\%$ ) (**Figure S8**).

368  
369 CrAssphage, PMMoV, and *Bacteroides* rRNA were quantifiable in all samples tested, but 18S  
370 rRNA was below the LoD for 24% of samples. Furthermore, 18S rRNA was the only biomarker  
371 that amplified in the extraction negative controls (75%) at similar levels as the samples ( $p>0.05$ ;  
372 **Figure S9**), which suggests that this target could be a common laboratory contaminant. Based  
373 on our findings that 18S rRNA was frequently detected in negative controls, inconsistently  
374 detected in sewage, and had high spatial and temporal variation in per capita shedding, we  
375 conclude that human 18S rRNA is not suitable as a normalization biomarker to adjust for fecal  
376 content.

377  
378 We suspected that lower biomarker concentrations (**Figure 1**), frequently undetected 18S rRNA  
379 (**Figure S9**), and high variability in N1 signal in location E samples reflected RNA degradation

380 because: (i) location E is the largest sewershed in the study (i.e., longer residence time allowing  
381 for signal degradation); and (ii) some samples from this site thawed during transportation back to  
382 the lab (resulting in an additional freeze-thaw cycle, which could degrade RNA (Ahmed et al.,  
383 2020c; Coryell et al., 2020)). Data from sewershed E was not used for subsequent analyses  
384 because of the uncertainty surrounding the integrity of these samples.

385

### 386 **3.2 SARS-CoV-2 N1 and clinical testing data were correlated and some normalization** 387 **biomarkers maintained this relationship**

388 The SARS-CoV-2 N1 concentration in wastewater was moderately correlated to daily per capita  
389 clinical cases when aggregated across all locations ( $\tau=0.43$ ,  $p<0.0001$ ; **Figure 2**). However, there  
390 are several limitations to assessing correlation between clinical testing data and wastewater data.  
391 First, clinical testing data do not necessarily represent true incidence because of biases  
392 associated with testing. Even if clinical and wastewater testing data correspond to the same date,  
393 fecal shedding could peak before symptom onset, which would impact the correlation unless the  
394 correct time offset is applied to reflect this discrepancy (Hoffmann and Alsing, 2021). Additionally,  
395 for this analysis, clinical and wastewater testing data would ideally both correspond to the sample  
396 collection date (as opposed to the result date) to remove lag introduced by test result turnaround  
397 time (see section 3.3 for more information). However, often only one date was available for clinical  
398 testing. For example, in this analysis, the only date associated with the daily per capita cases  
399 from most locations (all but K) was the date that the testing results were provided (result date),  
400 while the date associated with the SARS-CoV-2 N1 wastewater signal was the sample collection  
401 date.

402

403 Despite these potential limitations, correlation to daily per capita COVID-19 cases was used as a  
404 metric to assess the effect of normalization to biomarkers (crAssphage, PMMoV, and *Bacteroides*  
405 rRNA). Moderate, significant correlations were observed with COVID-19 daily per capita cases

406 when SARS-CoV-2 N1 was unnormalized and normalized by crAssphage or *Bacteroides*  
407 ( $\tau_{\text{unnormalized}}=0.43$ ,  $\tau_{\text{crAssphage}}=0.38$  and  $\tau_{\text{Bacteroides}}=0.35$ ,  $p<0.0001$ ; **Figure 2**); however, normalization  
408 did not strengthen the correlation compared to unnormalized signal. Conversely, PMMoV  
409 normalization produced only a weak correlation of 0.18 ( $p < 0.05$ ) (**Figure 2**). Analysis was  
410 performed with and without samples that were below the limit of detection and produced similar  
411 results (**Table S11**). Of the normalization biomarkers tested, crAssphage had the lowest variability  
412 and also maintained significant and moderate correlation with clinical testing data, so we included  
413 it in subsequent analyses alongside unnormalized concentrations.

414  
415 The correlation analysis was repeated with data separated by location to determine whether  
416 locational dependencies affect the relationship between wastewater and clinical testing data as  
417 well as the performance of normalization strategies. Locations with at least 75% of data above  
418 the N1 qPCR LoD (Locations K, N, and S; **Table S12**) were included in this analysis. Only location  
419 K had significant correlations with clinical testing data, both with and without crAssphage  
420 normalization ( $\tau_{\text{unnormalized}}=0.5$  and  $\tau_{\text{crAssphage}}=0.43$ ,  $p<0.05$ ; **Figure S10**). This finding suggests  
421 locational dependencies (e.g., differences in extent of clinical testing, sewer system residence  
422 times, etc.) affect the correlation with clinical testing data. Additionally, the location-specific  
423 analysis was repeated including only samples with detectable SARS-CoV-2 N1 signal, and the  
424 results were no longer statistically significant (**Figure S10**). This finding is likely influenced by both  
425 the limited sample size and values below the N1 qPCR LoD that affect rank correlations.

426  
427 In addition to the limitations in clinical testing data mentioned at the beginning of this section,  
428 there are several explanations for why wastewater signal at locations S, N and K did not  
429 significantly correlate with clinical testing data after removing values below the LoD: (i) the daily  
430 per capita cases in the population were at or below the WBE case detection limit of the wastewater  
431 data; (ii) the daily per capita cases that were masked by public health departments for patient



432 privacy impaired the rank correlation analysis by left-censoring the clinical testing data; (iii) the  
433 wastewater signal did not vary enough over the time of sampling to establish rank. The possibility  
434 that the wastewater signal leads the clinical testing data was subsequently tested for locations K,  
435 N, and S (i.e., correlations were examined for zero-, one-, and two-week offsets); however,  
436 location K was the only location with significant correlation between wastewater and clinical  
437 testing data for any lead time tested (**Figure S10**).

438

### 439 **3.3 Impact of the date associated with clinical testing data on lead time in wastewater** 440 **surveillance at location K**

441 The time for laboratories to process samples and return results (testing turnaround time) affects  
442 the potential for wastewater surveillance to provide lead time over clinical surveillance. In general,  
443 clinical testing data correspond to either the date the sample was collected or the date the results  
444 were returned. The ideal date to use for informing public health decisions would be the result date,  
445 to include differences between clinical and wastewater testing turnaround time in the analysis.  
446 Alternatively, sample collection dates should be compared to understand the timing of the  
447 underlying biological mechanisms that result in a positive wastewater signal (onset and duration  
448 of fecal shedding) and positive clinical test (onset and duration of nasopharyngeal shedding).  
449 Onset and duration of symptoms may influence the timing of the clinical test (sample collection  
450 date), depending on whether testing is routine or only available to symptomatic individuals.  
451 Hence, the ideal date to use for comparison of wastewater and clinical testing data differs  
452 depending on the goals of the comparison. The clinical testing data for location K included sample  
453 collection date, result date, and episode date (the earliest date associated with the case), allowing  
454 us to assess the correlation between case data and wastewater data with and without clinical  
455 testing turnaround time. Episode date was frequently the same as the sample collection date,  
456 unless a patient reported symptoms prior to test date (**Figure S11**). It should be noted that  
457 wastewater testing data correspond to the sample collection date because all samples were

458 processed retroactively in this study. Routine wastewater testing turnaround time can be 1-3 days  
459 but could vary depending on sample transport and laboratory methods (“Covid-WEB,” n.d.).

460  
461 To test the influence of the date associated with clinical testing, we repeated correlation analysis  
462 for location K (**Figure S11**). The wastewater testing data (sample collection date) correlated with  
463 the clinical testing data by episode date ( $\tau_{\text{episode,unnormalized}}=0.56$ ,  $\tau_{\text{episode,crAssphage}}=0.54$ ,  $p<0.01$ ) and  
464 sample collection date ( $\tau_{\text{collection,unnormalized}}=0.59$ ,  $\tau_{\text{collection,crAssphage}}=0.62$ ,  $p<0.01$ ) without a lead or  
465 lag. When the result date was used for clinical testing data, the strongest correlation with  
466 wastewater data was associated with a two-week lead time (unnormalized N1 concentration) or  
467 one-week lead time (N1 normalized to crAssphage; **Figures S10** and **S11**). When values below  
468 the N1 qPCR LoD were removed, wastewater data were no longer significantly correlated with  
469 episode date-associated clinical data, but the strongest correlations for the other date  
470 associations remained significant. This analysis is limited because of the small dataset, but the  
471 methodology presented here can be used to assess the lead time provided by wastewater  
472 surveillance with larger data sets and with wastewater data processed contemporaneously with  
473 decision-making.

474  
475 **3.4 The Lowess bandwidth parameter affected wastewater data trend interpretation**

476 Variation in wastewater SARS-CoV-2 N1 signal from sources other than variation in true incidence  
477 or prevalence (e.g., noise introduced during sample collection, processing, etc.) can obscure  
478 temporal trends. Smoothing techniques can be used to visually distinguish temporal trends from  
479 noise. Similar to the choice of the number of days included for each average calculation for moving  
480 averages (window), Lowess requires selection of the fraction of the whole time series that is used  
481 for each local regression calculation (bandwidth). We employed a method to set the bandwidth  
482 parameter systematically based on residuals (Jacoby, 2000) independently for each location. The  
483 bandwidth was increased stepwise, beginning with inclusion of one point in each local regression

484 calculation and ending with inclusion of all points ( $\alpha=1$ ). For each bandwidth value, the residuals  
485 were calculated and plotted by date, and a Lowess trendline with  $\alpha=1$  was fit to these residual  
486 plots to monitor residual trends as the bandwidth varied. Finally, the maximum bandwidth value  
487 was selected for which the residuals visually maintained horizontal Lowess trendlines (see  
488 **Figures 3 and S2-S5**).

489  
490 As an example, for unnormalized and crAssphage-normalized SARS-CoV-2 N1, bandwidth  
491 parameters of 0.39 and 0.33 were respectively chosen for location N (**Figure 3 A**). This process  
492 was repeated for all locations, and bandwidths in the range of 0.25-0.6 were selected based on  
493 the optimization procedure (see **Figures 3 and S2-S5**). To assess the impact of bandwidth on  
494 SARS-CoV-2 N1 signal interpretation, Lowess was performed for all locations sampled and for all  
495 possible bandwidths (see **Figures 3 B and S2-S5**). The bandwidth parameter influenced the  
496 overall temporal trends of wastewater data for some locations (N and A; **Figures 3 and S5**). For  
497 example, at location A (**Figure S5**), a bandwidth of 1 resulted in a gradual increase in SARS-CoV-  
498 2 N1 signal during sampling, while a bandwidth of 0.73 resulted in a peak around July. However,  
499 for location K (**Figure S2**), all bandwidths resulted in trends that would have similar  
500 interpretations. These results illustrate that choice of bandwidth could have implications for  
501 interpreting WBE data and informing COVID-19 response strategies, and systematic methods  
502 should be used to select the appropriate bandwidth.

503  
504 **3.5 Wastewater and clinical data had similar overall trends regardless of normalization,**  
505 **with notable exceptions**

506 To assess the impact of crAssphage normalization on SARS-CoV-2 N1 temporal trends, we  
507 compared unnormalized and crAssphage-normalized Lowess trendlines (**Figure 4**). We found  
508 that crAssphage-normalized trends were similar to unnormalized trends for three of the locations  
509 (K, N, and A) but had differences in overall trend for locations Q (**Figure 5**) and S (**Figure S12**).

510 Discrepancies are concerning because they could have implications for pandemic response. We  
511 note that the trend in location K, for which biological replicates were processed routinely, was the  
512 least impacted by bandwidth or normalization (**Figures S2 and S12**). Larger datasets with more  
513 frequent sampling and processing of biological replicates, would give single points less influence  
514 over the trend.

515  
516 Relative spatio-temporal trends in clinical and wastewater testing results were compared across  
517 sampling sites (**Figures 4, S6, and S7**). In general, clinical and wastewater data at all locations  
518 paralleled one another, with San Quentin prison (Q) showing the highest COVID-19 burden  
519 across locations. Due to a COVID-19 outbreak, location Q had a maximum that was 53 times  
520 (SARS-CoV-2 N1  $4.89 \times 10^3$  gene copies/mL), 17 times (crAssphage-normalized SARS-CoV-2  
521 N1 ratio  $2.9 \times 10^{-3}$ ), and 203 times ( $\sim 85$  new cases per 1000 people on 6/29) higher than the  
522 highest value at the sewershed scale. There were a few discrepancies between clinical and  
523 wastewater trends (heatmap visualizations in Figures S6 and S7 highlight discrepancies in  
524 peaks). For example, at location N, there may have been clinical undertesting, based on the peak  
525 in wastewater data in August (**Figures 4 and S6**) and higher SARS-CoV-2 signal in wastewater  
526 at location N (relative to other locations) than represented by the clinical data (**Figures 4 and S7**).

527

### 528 **3.6 The WBE case detection limit was estimated to be 2.4 COVID-19 cases per 100,000** 529 **people**

530 Quantifying the minimum per capita new COVID-19 cases in a sewershed at which there is  
531 reliable detection of SARS-CoV-2 N1 in wastewater (WBE case detection limit) is important for  
532 gauging the utility of COVID-19 WBE when the true incidence is low. This WBE case detection  
533 limit depends on the detection limit of the wastewater measurement (i.e., the methods used to  
534 store, concentrate, extract, and measure SARS-CoV-2 RNA in wastewater) and the accuracy of  
535 the clinical testing data available. To estimate the WBE case detection limit in a way that is

536 replicable across studies, the cumulative percentage of amplified technical replicates of the  
537 wastewater data for inversely-ranked daily per capita COVID-19 cases was fit to a logistic growth  
538 model (without samples associated with masked case values; see Methods). When COVID-19  
539 case rates equaled or exceeded 2.4 daily cases per 100,000 people, 95% of wastewater technical  
540 replicates amplified via RT-qPCR for N1 (**Figure 6**). Other researchers have used non-cumulative  
541 methods to estimate the WBE case detection limit by calculating the percent of amplified  
542 wastewater replicates for each case value (Wu et al., 2021). This method requires repeated  
543 wastewater measurements associated with each possible clinical case value or range of case  
544 values (i.e., bins). Otherwise, the percent of amplified technical replicates is limited, as was the  
545 case in this study where only one biological replicate was often associated with each case number  
546 (**Figure S13 A**). Ideally, all data would be unmasked when applying this method. To verify that  
547 the masked clinical data did not affect the estimated WBE case detection limit, the process was  
548 repeated with masked values, and the estimate was similar (2.2 cases in 100,000 people; **Figure**  
549 **S13 B**). These limits are within the theoretical range possible (Hart and Halden, 2020b) and similar  
550 in magnitude to previous findings of 10 in 100,000 (Hata and Honda, 2020) and 13 in 100,000  
551 (Wu et al., 2021).

552  
553 Based on the contributing population of each sewershed in this study, the WBE case detection  
554 limit translates to 11.6 cases for K, 11.3 cases for S, 3.3 cases for N, 2.0 cases for A, and 0.1  
555 cases for Q. Therefore, at location Q, one case should be reliably detected based on results from  
556 this analysis, which could be tested observationally because only one new case was detected by  
557 clinical testing after August 12<sup>th</sup> (**Figure 5**) with the test results provided on 8/26. When  
558 wastewater sampling was completed on 8/25 and 9/1, a weak positive signal was observed (one  
559 technical replicate amplified). These results support that wastewater testing can detect clinical  
560 cases in facilities with a single case; however, to capture a strong positive signal from one case  
561 at a facility, higher frequency sampling is recommended. A possible explanation for why a single

562 case may still go undetected, despite being above the WBE case detection limit, is that  
563 wastewater surveillance relies on the autosampler aliquots capturing the feces from each infected  
564 individual, which becomes less likely when there are fewer infected individuals and wastewater  
565 has less mixing prior to the sampling location. These results are promising for the application of  
566 WBE in facilities, where it is highly resource-intensive to conduct routine clinical surveillance  
567 testing frequently enough to detect a single case in time to enact preventative measures. More  
568 work is needed applying WBE for SARS-CoV-2 across a broader set of facilities.

569

## 570 **4. DISCUSSION**

571

### 572 **4.1 Validation and potential use scenarios of SARS-CoV-2 wastewater testing**

573 During the COVID-19 pandemic, both the methodological research for SARS-CoV-2 testing in  
574 wastewater and the application of WBE have been occurring simultaneously. For COVID-19 WBE  
575 to be useful for public health decision-making, public health officials need to be confident that the  
576 resulting SARS-CoV-2 signal reflects COVID-19 trends in the contributing population. Despite  
577 limitations in clinical testing data and the potential lag in wastewater trends, assessing correlations  
578 between clinical and wastewater testing data can help validate WBE (Xagorarakis and O'Brien,  
579 2020). Moderate correlations with clinical data observed in this study ( $\tau=0.43$ ) support that trends  
580 in wastewater surveillance data reflect trends in COVID-19 disease occurrence. Wastewater data  
581 paired with clinical data can be a more robust public health surveillance strategy compared to  
582 either method alone, both for sewershed-scale and facility-scale surveillance applications. In  
583 some settings, wastewater testing may be a less resource-intensive way to implement population-  
584 scale surveillance, and policymakers will need to balance allocation of resources to each  
585 approach.

586

587 A critical question for public health decision-making is how much early warning WBE can provide  
588 ahead of clinical testing, which could allow more timely public health responses to slow COVID-  
589 19 outbreaks. However, lead time is difficult to measure. Biologically, the time between onset of  
590 fecal shedding and nasal shedding is unclear (Benefield et al., 2020; Walsh et al., 2020).  
591 Practically, lead time depends on testing turnaround time and frequency of sampling for both  
592 wastewater and clinical testing. For example, clinical testing capabilities can increase the lead  
593 time of wastewater data if patients are only tested after symptom onset and can decrease the  
594 lead time if asymptomatic and symptomatic individuals are regularly screened with rapid  
595 turnaround time. Ideal assessments of wastewater data lead time due to biological mechanisms  
596 would not include turnaround time, whereas assessments of the performance of clinical and  
597 wastewater laboratories for public health action and practical limitations would include turnaround  
598 time. Although other studies observed lead time for wastewater data over clinical data starting on  
599 the order of days (D'Aoust et al., 2021a; Nemudryi et al., 2020; Peccia et al., 2020, the weekly  
600 sampling in our study could explain why no lead time was determined when the sample collection  
601 date was used for both wastewater and clinical testing data (**Figure S14**). However, the impact  
602 of clinical testing strategy (i.e., only screening symptomatic individuals) could also be affecting  
603 this result. We could not directly compare wastewater and clinical result dates in this retroactive  
604 study, but when clinical data were associated with the result date and wastewater data were  
605 associated with sample collection date, lead time of 1-2 weeks was observed (**Figure S14**). Other  
606 researchers have observed lead time in wastewater data of up to three weeks (Ahmed et al.,  
607 2021; Medema et al., 2020), and our results reflect a similar range in possible lead times (0-2  
608 weeks) depending on which date is associated with the clinical data.

609  
610 At the sewershed scale, the benefit of WBE to public health extends beyond early warning.  
611 Discrepancies between wastewater testing data and clinical testing data trends from early in the  
612 time series at location N (April-July 2020; **Figure S12**) could be used to infer clinical undertesting,

613 which is supported by lower testing capacity in this time frame (**Figure S15**). Although pairing  
614 COVID-19 clinical testing data with wastewater SARS-CoV-2 data can generate new insights for  
615 public health decision-making, it can be challenging in practice. Pairing wastewater SARS-CoV-  
616 2 data with geocoded COVID-19 clinical testing data required collaboration between academics,  
617 wastewater treatment facility representatives, and public health officials. These collaborations  
618 may be particularly difficult at sewershed-scale, where multiple public health department  
619 jurisdictions overlap (e.g., location N). Partnerships for data sharing between agencies are critical  
620 to support ongoing wastewater-based epidemiology for SARS-CoV-2 and other pathogens.

621  
622 At the facility scale, monitoring raw wastewater for SARS-CoV-2 might be particularly useful for  
623 early detection of COVID-19 outbreaks. San Quentin Prison (location Q) had a COVID-19  
624 outbreak during the study period after a transfer from the California Institution for Men (Cassidy  
625 and Fagone, 2020), where, at its peak, 47% of the population had active cases. The maximum  
626 SARS-CoV-2 N1 concentration ( $4.89 \times 10^3$  gene copies/mL) was higher than any sewershed  
627 sampled in this study and among the highest values we found in the literature for N1 in raw  
628 wastewater (Gerrity et al., 2021; Gonzalez et al., 2020; Medema et al., 2020; Randazzo et al.,  
629 2020b; Wu et al., 2020; Wurtzer et al., 2020), despite regular clinical testing (**Figure S15**). Prison  
630 conditions cause incarcerated people to be particularly susceptible to respiratory disease  
631 outbreaks, and maintaining safety in prisons requires deliberate planning and coordination by  
632 correctional institutions (e.g., coordination with local public health systems to develop pandemic  
633 response plans, coordination of transfers between institutions, etc.) (Montoya-Barthelemy et al.,  
634 2020). Furthermore, the health of incarcerated people is linked to the health of the community,  
635 and incorporating correctional institutions into community safety plans will help ensure better  
636 protection against COVID-19 for everyone (Montoya-Barthelemy et al., 2020). Once protective  
637 measures are implemented, WBE may be useful to monitor prisons and other high-risk facilities



638 (e.g., skilled nursing facilities, homeless shelters, etc.), especially where clinical testing is not  
639 available or routine.

640

## 641 **4.2 Approaches for translatable WBE**

642

### 643 **4.2.1 Normalization of wastewater targets to adjust for fecal content**

644 Results from this study suggest that PMMoV, *Bacteroides* rRNA, and 18S rRNA were less  
645 promising normalization biomarkers than crAssphage. While PMMoV was present in high and  
646 stable concentrations, the diet-dependency (Symonds et al., 2019) and large range in  
647 concentrations in the literature (six orders of magnitude; **Table S10**) remain concerns for its use  
648 over longer time scales and across larger geographic regions. Normalization to PMMoV resulted  
649 in the weakest significant correlation to clinical testing data of the biomarkers tested ( $\tau=0.18$ ,  
650  $p<0.05$ ), in contrast to other studies that found normalization to PMMoV improved correlation with  
651 clinical data (D'Aoust et al., 2021b; Wu et al., 2020). *Bacteroides* rRNA loads varied more spatially  
652 and temporally than crAssphage or PMMoV in this study (**Figure 1**), but *Bacteroides*-normalized  
653 SARS-CoV-2 N1 had a moderate correlation with clinical testing data ( $\tau=0.35$ ). While  
654 measurement of *Bacteroides* rRNA gene in wastewater has been commonly applied for fecal  
655 source tracking and *Bacteroides* rRNA has been targeted to increase assay sensitivity (D'Aoust  
656 et al., 2021b; Feng et al., 2021), to our knowledge, no prior raw wastewater values have been  
657 reported in the literature for *Bacteroides* rRNA (**Table S10**). Similarly, no values were found in the  
658 literature for 18S rRNA concentrations in raw wastewater (**Table S10**). In this study, 18S rRNA  
659 signal displayed a wide range in concentrations and consistently amplified in negative extraction  
660 controls. Furthermore, 18S rRNA was less stable in wastewater than SARS-CoV-2 RNA and  
661 nonenveloped viruses (e.g., crAssphage and PMMoV), which is consistent with previous studies  
662 (Whitney et al., 2021; Wurtzer et al., 2020). Therefore, we do not recommend 18S rRNA use as  
663 a normalization biomarker. In comparison to all of the biomarkers tested, crAssphage had low

664 spatial variability (i.e., the fewest locations with statistically different loads; **Figure 1**) and temporal  
665 variability (gCV=59%; **Figure 1**). Additionally, normalized SARS-CoV-2 N1 correlated with daily  
666 per capita COVID-19 cases ( $\tau=0.38$ ). Although crAssphage concentrations in the literature had a  
667 wide range (six orders of magnitude; **Table S10**), they were consistent across locations in this  
668 study. Based on this dataset, crAssphage remains a promising endogenous normalization  
669 biomarker for broader WBE applications.

670

671 Although a standardized approach would facilitate comparisons across studies, the ideal  
672 normalization strategy may be situationally dependent. For example, in this study, for some  
673 locations, crAssphage-normalization did not have a major impact on general spatio-temporal  
674 trends and did not improve correlations to clinical data compared to unnormalized signal, likely  
675 due to the lack of precipitation or changes in flow throughout the study period. Several factors  
676 should be considered when deciding whether to normalize to a biomarker or report unnormalized  
677 concentrations. First, adding another assay introduces additional analytical variation that could  
678 outweigh the benefits of biomarker normalization in some settings (Feng et al., 2021). An  
679 additional consideration is ensuring methods compatibility with the WBE target and normalization  
680 biomarker. Ideally, normalization to an endogenous biomarker would account for losses in target  
681 signal during residence time in sewers, sample storage, and laboratory processing, but the ideal  
682 biomarker for fecal content may not be the best surrogate for the target of interest. For example,  
683 crAssphage is not expected to be a good surrogate for SARS-CoV-2 stability, partitioning, and  
684 extraction (Ye et al., 2016), and as a DNA virus, crAssphage may be incompatible with some  
685 extraction methods used for SARS-CoV-2 RNA. Other controls (e.g., endogenous biomarkers,  
686 recovery controls) and modeling may be applied to improve measurement accuracy and translate  
687 results across labs and methods, although there are challenges associated with these corrections  
688 (Kantor et al., 2021). Degradation modeling with target-specific decay constants (Ahmed et al.,

689 2020a) and sewershed-specific parameters could assist in correcting for degradation or  
690 determining sample integrity, but no comprehensive approach for this correction exists.

691

#### 692 **4.2.3 A systematic approach for data smoothing (Lowess)**

693 In general, public health decisions are based on temporal trends in disease burden, not individual  
694 data points, but trends in wastewater and clinical data can be difficult to visually distinguish,  
695 especially when available resources constrain sampling frequencies. Applying Lowess to  
696 wastewater data, we found that the value of one parameter could influence the trend visualization  
697 such that the same dataset could lead to different public health responses (**Figures 3 and S5**).  
698 Based on our analysis, the bandwidth parameter for Lowess should be determined for each  
699 sewershed sampled. Lowess with a systematically chosen bandwidth could be used to smooth  
700 trendlines and minimize the loss of temporal resolution. The method presented here could be  
701 applied in retrospective analysis or in real-time analysis completed as part of wastewater public  
702 health surveillance programs. For real-time applications, the bandwidth parameter could be  
703 selected using a subset of data, and the residuals plot could be frequently checked to ensure no  
704 new residual patterns emerge over time that could obscure the smoothed trend.

705

#### 706 **4.2.4 A systematic approach to estimate a WBE case detection limit**

707 In addition to data smoothing, we developed an approach for identifying a WBE case detection  
708 limit that can be applied systematically to studies using PCR-based methods. We applied this  
709 analysis to SARS-CoV-2 N1 signal in wastewater and found that the daily new clinical cases at  
710 which wastewater surveillance could reliably detect clinically diagnosed COVID-19 cases in the  
711 contributing population was estimated at 2.4 cases per 100,000 people. There are multiple  
712 limitations to this analysis because wastewater detection depends on factors other than incidence,  
713 such as sampling methods (e.g., frequency of sampling aliquots), which can influence the  
714 probability of capturing shed viral particles from an infected individual. Additionally, the estimate

715 may vary based on site-specific clinical testing availability, wastewater sampling methods (e.g.,  
716 composite sampling, freezing before processing) and laboratory processing (e.g., 4S extraction  
717 method, RT-qPCR). The estimation method for a WBE case detection limit presented here could  
718 benefit both COVID-19 WBE and other disease WBE by providing a systematic method to  
719 compare the case detection limits across studies.

720

## 721 5. CONCLUSION

722 • Wastewater N1 concentrations had a moderate correlation with geocoded clinical testing  
723 data ( $\tau_{\text{unnormalized}}=0.43$ ). Normalization of SARS-CoV-2 N1 signal in wastewater to any  
724 biomarker did not improve the correlation with clinical testing data, likely because of the  
725 low variation in daily flow rates.

726 • Of the normalization biomarkers tested, crAssphage was the most promising due to low  
727 spatial and temporal variability and because crAssphage-normalized N1 had the strongest  
728 correlation with clinical testing data ( $\tau_{\text{crAssphage}}=0.38$ ,  $\tau_{\text{Bacteroides}}=0.35$ ,  $\tau_{\text{PMMoV}}=0.18$ ).

729 • 18S rRNA was not suitable as a normalization biomarker due to its variability in sample  
730 concentrations, high degradation rate, and ubiquity as a laboratory contaminant.

731 • There was evidence of clinical undertesting at location N, which supports that wastewater  
732 testing could provide insights about COVID-19 trends in the population when clinical  
733 testing capabilities are limited.

734 • The COVID-19 outbreak at San Quentin prison (location Q) corresponded to a measured  
735 N1 concentration that was higher than any sewershed tested ( $4.89 \times 10^3$  gene copies/mL).

736 • The wastewater-based epidemiology case detection limit using the 4S RNA extraction  
737 method on frozen samples was estimated to be 2.4 COVID-19 cases in 100,000 people.

738 • Lead time in wastewater over clinical testing varied from 0 to 3 weeks depending on the  
739 location, biomarker normalization, and testing turnaround time.

740 • Systematic approaches for determining a WBE case detection limit, biomarker

741 normalization, and trendline smoothing were presented that can be applied across future  
742 WBE studies.

743

744

745

746

747

748

749

750

751

752

753

754

755

756

757

758

759

760

761

762

763

764

765

766

767

**FIGURES AND TABLES**

768

769

770

771

772

**Table 1:** Descriptions of wastewater sampling locations including associated wastewater utility, clinical testing data sources, population, and flow rates. “d” represents the number of unique dates on which samples were collected. “n” represents the total number of wastewater samples collected, including biological replicates.

<b>Wastewater catchment area</b>	<b>Wastewater treatment facility</b>	<b>COVID-19 clinical data source</b>	<b>Population</b>	<b>Mean flow rate (MGD)</b>	<b>Mean per capita flow (L/person/day)</b>	<b>d</b>	<b>n</b>
<b>Location K</b> Influent to the wastewater treatment facility	Central Contra Costa Sanitary District	Contra Costa County Public Health Department	483,600	33	261	13	39
<b>Location S</b> Upstream of wastewater treatment facility	East Bay Municipal Utility District	Alameda County Public Health Department	469,344	35	282	20	22
<b>Location A</b> Upstream of wastewater treatment facility	East Bay Municipal Utility District	Alameda County Public Health Department	82,818	6	274	11	17
<b>Location N</b> Upstream of wastewater treatment facility	East Bay Municipal Utility District	Contra Costa County and Alameda County Public Health Departments	139,037	10	272	18	18
<b>Location Q*</b> Wastewater collection point for San Quentin Prison	Central Marin Sanitation Agency	California Department of Corrections and Rehabilitation open data portal	Ranges from 3,587 (June) to 2,930 (September)	0.41	481	10	11
<b>Location E</b> Influent to the wastewater treatment facility	San Jose - Santa Clara Regional Wastewater Facility (SJSC-RWF)	Not applicable	1,500,000	103	278	19	48

773

774

\*For location Q, the population and clinical data are from people incarcerated only and do not include staff.

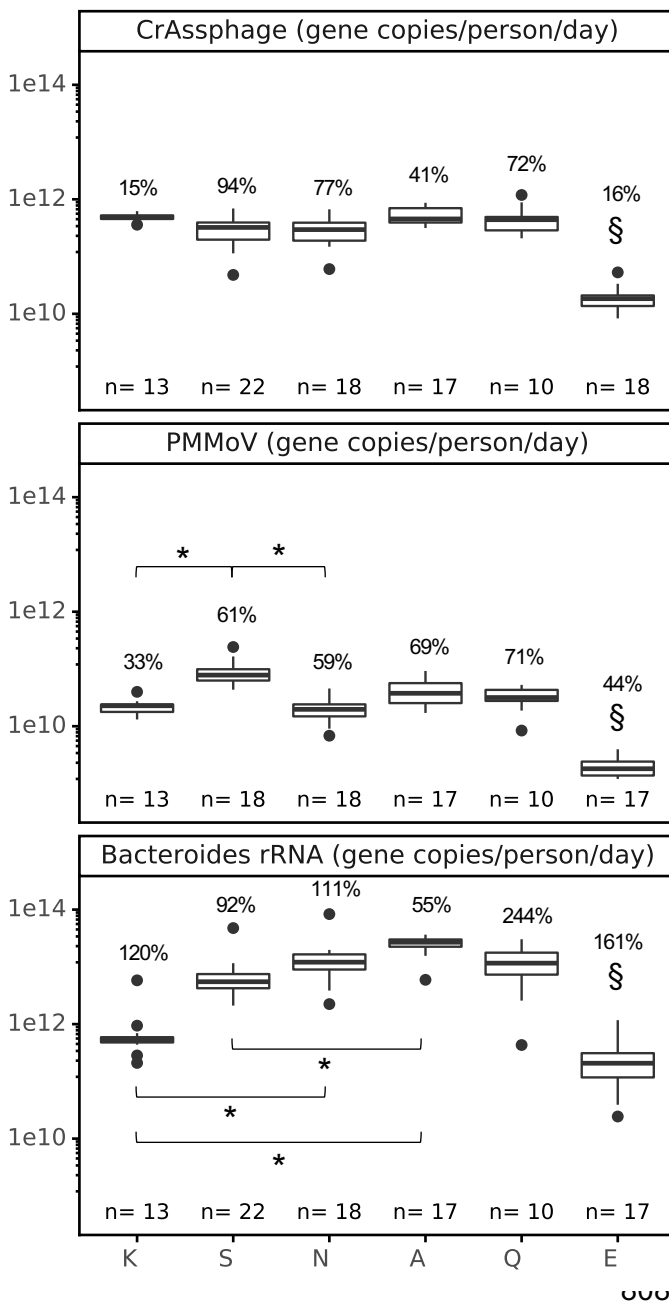


**Figure 1: Spatial and temporal variation in crAssphage, PMMoV, and *Bacteroides* wastewater loads.** Only one biological replicate per date per location is shown. 18S rRNA results were not included in the figure for consistency of scale due to the wide range in sample values and are included in the SI (**Figure S8**). The temporal variation within each location was assessed as the geometric coefficient of variation, displayed as a percentage above each box. The significance of differences between locations was assessed using a Kruskal-Wallis test with a Bonferroni correction followed by Dunn's test, where \* indicates p < 0.001 for bracketed relationships and § (above location E) indicates p < 0.001 for every pairwise location comparison to E, except p > 0.001 when compared to location E (for crAssphage and *Bacteroides*) and location N (for crAssphage).

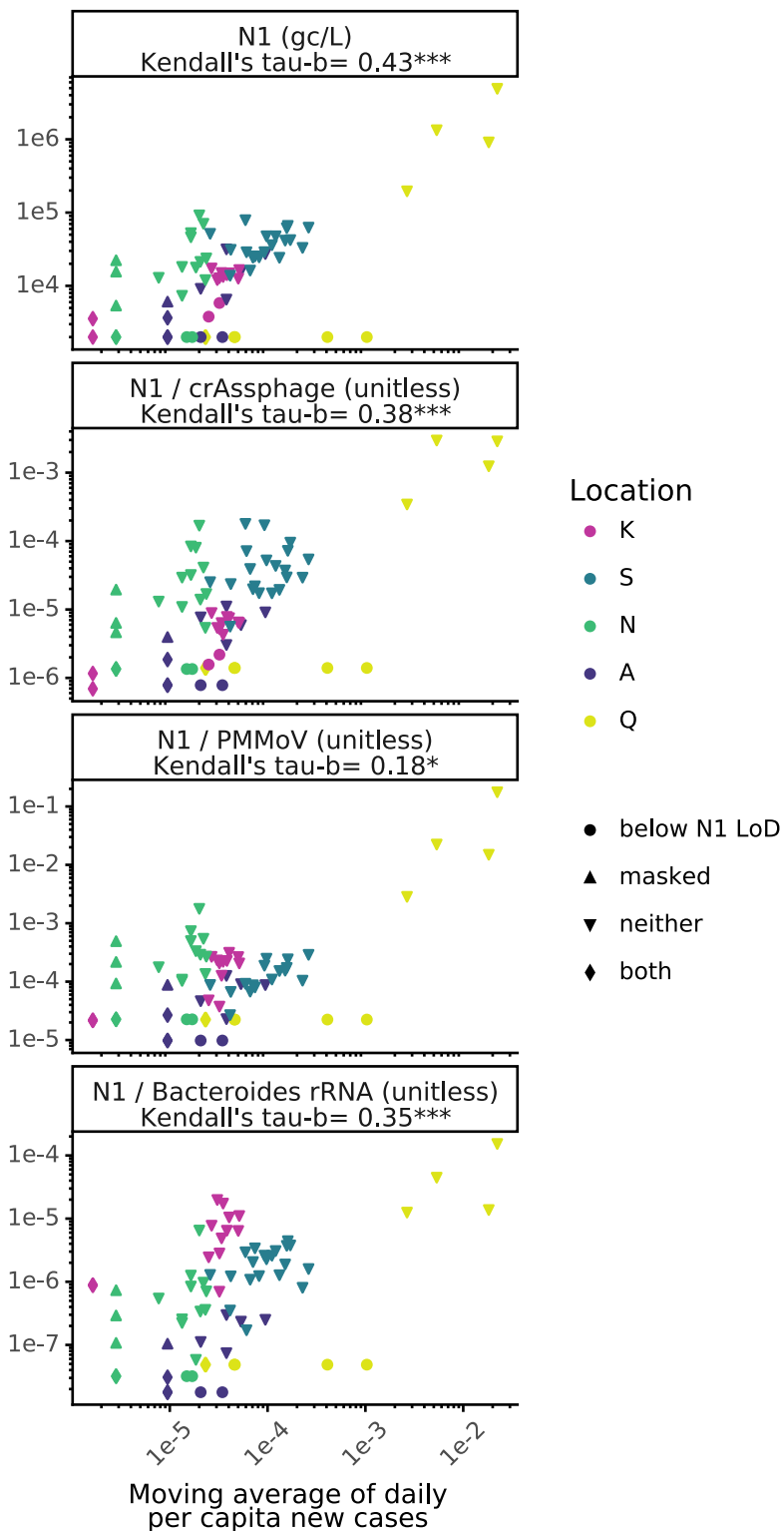
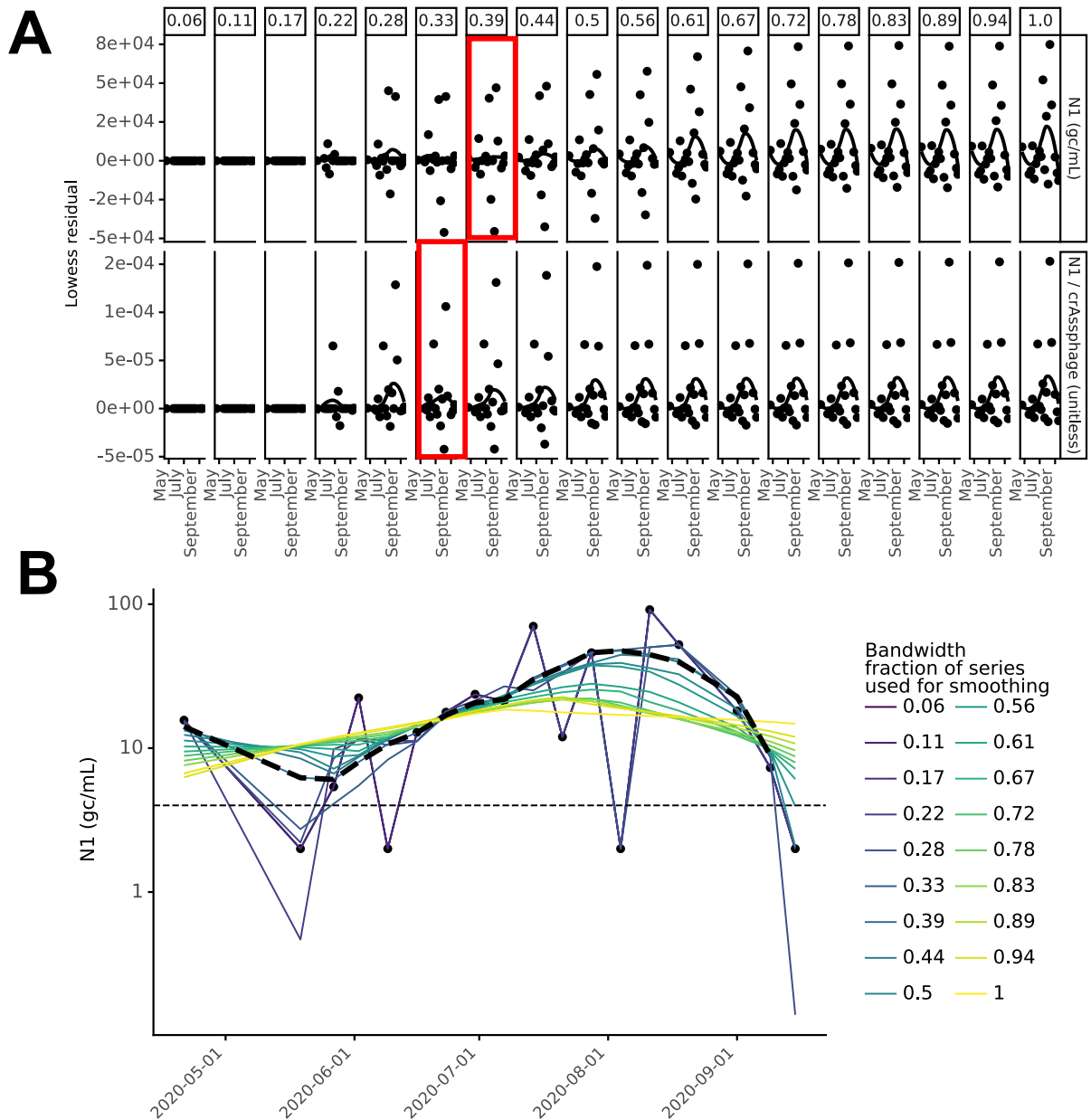
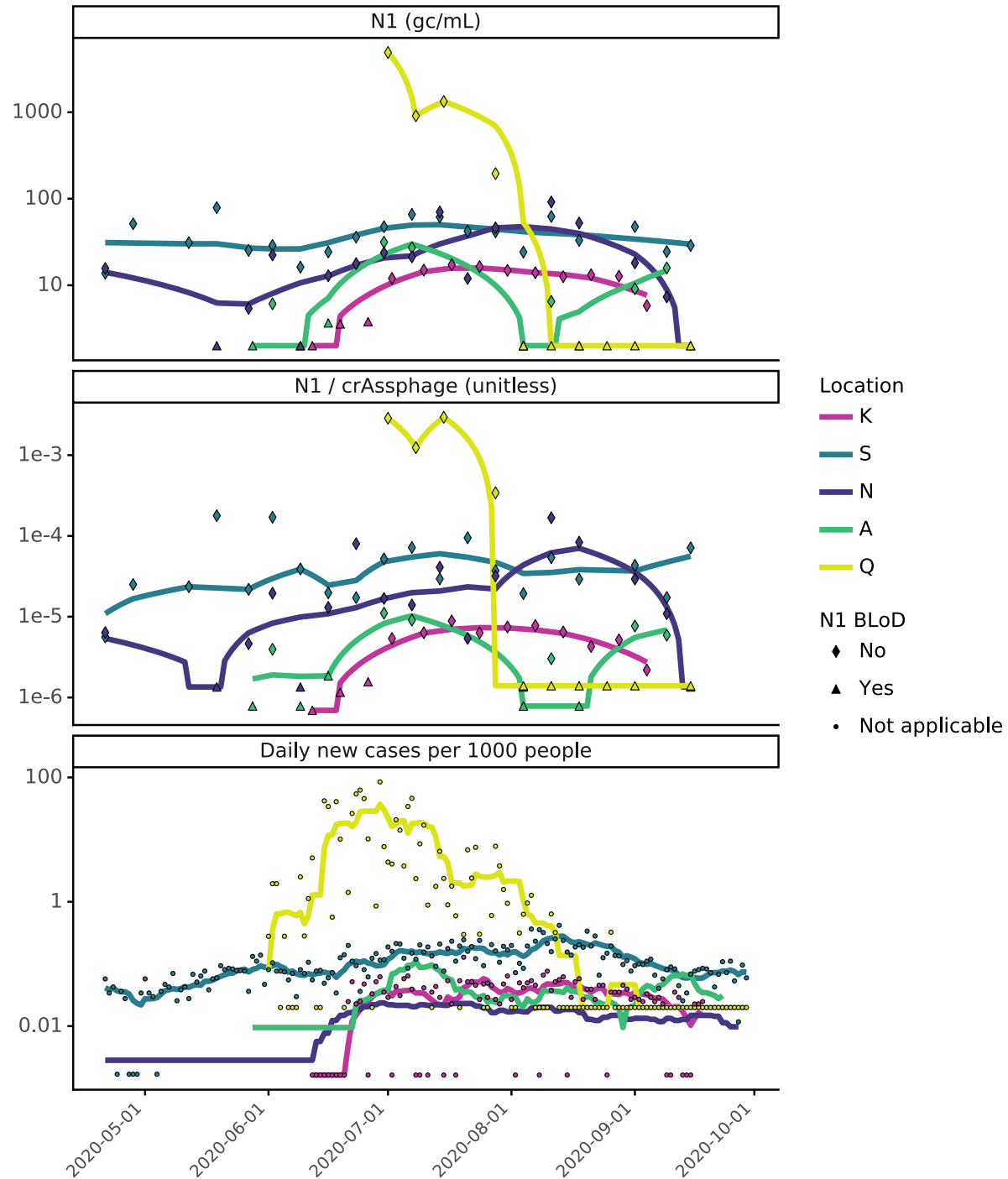


**Figure 2: Rank correlations of both unnormalized and normalized wastewater SARS-CoV-2 concentrations with clinical testing data.** N1 concentration, and N1 normalized proposed biomarkers are plotted against a seven-day moving average of new cases per capita per day for sample locations K, S, N, A, and Q. Shapes signify whether wastewater samples were below the qPCR limit of detection (LoD) for the N1 assay, associated with masked clinical case values, or both. Significance of rank correlation values in facet titles is indicated by \*= $<0.05$ , \*\*\*= $<0.0001$





850  
 851 **Figure 3: Example of Lowess bandwidth parameter selection process (Location N)**  
 852 (A) Residual plots for Lowess bandwidth parameter ( $\alpha$ ; column labels) determination for location  
 853 N where the bandwidth parameter increases from inclusion of 1 data point (far left) to inclusion  
 854 of all data points (far right) in each local regression for unnormalized N1 (top) and crAssphage-  
 855 normalized N1 (bottom). The value of  $\alpha$  that minimized the residual was selected (red boxes).  
 856 (B) Visualization of how bandwidth parameter affected the Lowess trendline for location N.  
 857 Black dashed line indicates the resulting Lowess trendline when  $\alpha=0.39$ .



858  
 859 **Figure 4: Comparison of wastewater SARS-CoV-2 N1 to geocoded COVID-19 clinical**  
 860 **testing results from May to September 2020.** Wastewater SARS-CoV-2 N1 signal is  
 861 compared as unnormalized (top) and crAssphage-normalized (middle), where lines are the most  
 862 optimal Lowess trendlines. COVID-19 clinical testing results are the daily per capita COVID-19  
 863 cases, where lines are the fourteen-day moving average (location N) or seven-day moving  
 864 averages (all other locations) (bottom). Heatmap visualization of the unnormalized N1 trendlines  
 865 is included in the SI (**Figures S6 and S7**) and visualization of sewersheds by location can be  
 866 found in **Figure S12**.

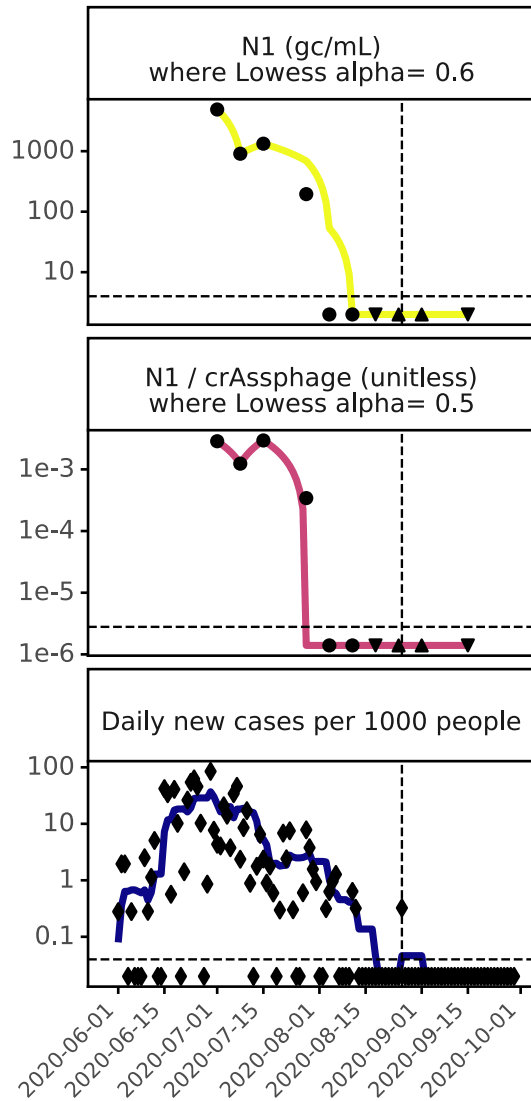
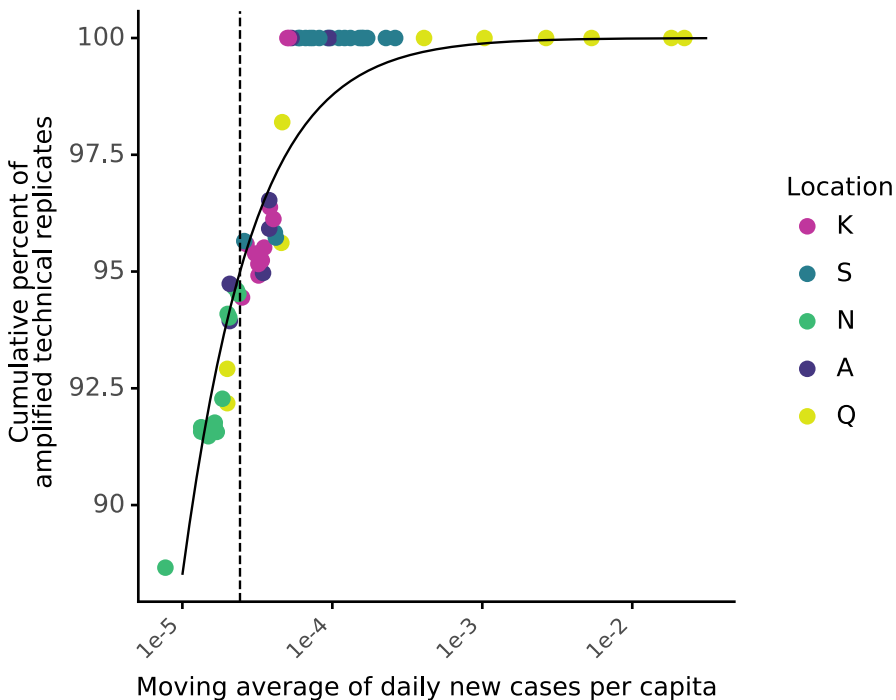


**Figure 5: Comparison of wastewater and clinical data at location Q from June to September 2020**, where

symbols indicate how many technical replicates amplified during qPCR. **Wastewater data :** (top) unnormalized and (middle) crAssphage-normalized SARS-CoV-2 N1 signal in wastewater, where the horizontal dashed line indicates the limit of detection, and trendlines are the most optimal Lowess trendline (Figure S4). **Clinical data (bottom):** daily per capita COVID-19 cases, where the horizontal dashed line indicates 1 case in 1000 people. Vertical dashed lines indicate August 26th, the only date after August 12th when a new COVID-19 case was detected at location Q through clinical surveillance.

Amplified technical replicates

- All
- ▲ Some
- ▼ None
- ◆ Not applicable



900  
901 **Figure 6: Estimated minimum number of COVID-19 clinical cases needed for reliable**  
902 **detection of SARS-CoV-2 RNA in wastewater.** The cumulative percentage of amplified  
903 wastewater technical replicates was calculated by ranking the moving averages of daily per  
904 capita cases (x-axis) from highest to lowest and calculating the fraction of qPCR replicates that  
905 amplified cumulatively (y-axis) for each value of x. The dashed line represents the daily new  
906 cases per capita value above which 95% of wastewater technical replicates amplified (2.4 cases  
907 in 100,000 people).

908  
909  
910  
911  
912  
913  
914  
915  
916  
917  
918  
919  
920  
921  
922  
923  
924  
925  
926

## ACKNOWLEDGEMENTS

We thank Matt Metzger, Melissa Thornton, and the whole COVID-WEB team for support. We also thank our wastewater utility partners for facilitating and assisting with wastewater sampling and physicochemical measurements, including from East Bay Municipal Utility District (Florencio Gonzalez, Bill Chan, Gabriela Esparza, Paula Hansen, Kiley Kinnon, Nick Klumpp, Debra Mapp, Christine Pagtakhan, Daniel Siu, Dave Williams, Zach Wu, and Cheryl Yee), Central Contra Costa Sanitary District (Lori Schectel, Mary Lou Esparza, Blake Brown, Amanda Cauble), San Jose-Santa Clara Regional Wastewater Facility (RWF) Operations and Laboratory staff, and Central Marin Sanitation Agency. We thank the COVID-19 WBE Collaborative (<https://www.covid19wbec.org/>) community for discussions of methods and approaches. Additionally, we thank Robert Tjian, Sarah Stanley, Erik Van Dis, Thomas Graham, and Mira Chaplin. We gratefully acknowledge funding from The Catena Foundation as well as rapid response grants from the Center for Information Technology Research in the Interest of Society and the Innovative Genomics Institute at UC Berkeley to K.L.N., H.D.G. and L.C.K. were supported by the National Science Foundation (NSF) Graduate Research Fellowship [grant number DGE-1752814]. In addition, H.D.G. was supported by the Berkeley Fellowship, and L.C.K. was supported by NSF INTERN through Re-Inventing the Nation's Urban Water Infrastructure [grant number: 28139880-50542-C].

927

## REFERENCES

- 928 Ahmed, W., Bertsch, P.M., Bibby, K., Haramoto, E., Hewitt, J., Huygens, F., Gyawali, P.,  
929 Korajkic, A., Riddell, S., Sherchan, S.P., Simpson, S.L., Sirikanchna, K., Symonds,  
930 E.M., Verhagen, R., Vasan, S.S., Kitajima, M., Bivins, A., 2020a. Decay of SARS-CoV-2  
931 and surrogate murine hepatitis virus RNA in untreated wastewater to inform application  
932 in wastewater-based epidemiology. *Environ. Res.* 191, 110092.  
933 <https://doi.org/10.1016/j.envres.2020.110092>
- 934 Ahmed, W., Bertsch, P.M., Bivins, A., Bibby, K., Farkas, K., Gathercole, A., Haramoto, E.,  
935 Gyawali, P., Korajkic, A., McMinn, B.R., Mueller, J.F., Simpson, S.L., Smith, W.J.M.,  
936 Symonds, E.M., Thomas, K.V., Verhagen, R., Kitajima, M., 2020b. Comparison of virus  
937 concentration methods for the RT-qPCR-based recovery of murine hepatitis virus, a  
938 surrogate for SARS-CoV-2 from untreated wastewater. *Sci. Total Environ.* 739, 139960.  
939 <https://doi.org/10.1016/j.scitotenv.2020.139960>
- 940 Ahmed, W., Bivins, A., Bertsch, P.M., Bibby, K., Choi, P.M., Farkas, K., Gyawali, P., Hamilton,  
941 K.A., Haramoto, E., Kitajima, M., Simpson, S.L., Tandukar, S., Thomas, K., Mueller, J.F.,  
942 2020c. Surveillance of SARS-CoV-2 RNA in wastewater: Methods optimisation and  
943 quality control are crucial for generating reliable public health information. *Curr. Opin.*  
944 *Environ. Sci. Health.* <https://doi.org/10.1016/j.coesh.2020.09.003>
- 945 Ahmed, W., Bivins, A., Bertsch, P.M., Bibby, K., Gyawali, P., Sherchan, S.P., Simpson, S.L.,  
946 Thomas, K.V., Verhagen, R., Kitajima, M., Mueller, J.F., Korajkic, A., 2020d. Intraday  
947 variability of indicator and pathogenic viruses in 1-h and 24-h composite wastewater  
948 samples: implications for wastewater-based epidemiology. *Environ. Res.* 110531.  
949 <https://doi.org/10.1016/j.envres.2020.110531>
- 950 Ahmed, W., Tschärke, B., Bertsch, P.M., Bibby, K., Bivins, A., Choi, P., Clarke, L., Dwyer, J.,  
951 Edson, J., Nguyen, T.M.H., O'Brien, J.W., Simpson, S.L., Sherman, P., Thomas, K.V.,  
952 Verhagen, R., Zaugg, J., Mueller, J.F., 2021. SARS-CoV-2 RNA monitoring in  
953 wastewater as a potential early warning system for COVID-19 transmission in the  
954 community: A temporal case study. *Sci. Total Environ.* 761, 144216.  
955 <https://doi.org/10.1016/j.scitotenv.2020.144216>
- 956 Been, F., Rossi, L., Ort, C., Rudaz, S., Delémont, O., Esseiva, P., 2014. Population  
957 Normalization with Ammonium in Wastewater-Based Epidemiology: Application to Illicit  
958 Drug Monitoring. *Environ. Sci. Technol.* 48, 8162–8169.  
959 <https://doi.org/10.1021/es5008388>
- 960 Benefield, A.E., Skrip, L.A., Clement, A., Althouse, R.A., Chang, S., Althouse, B.M., 2020.  
961 SARS-CoV-2 viral load peaks prior to symptom onset: a systematic review and  
962 individual-pooled analysis of coronavirus viral load from 66 studies. *medRxiv.*  
963 <https://doi.org/10.1101/2020.09.28.20202028>
- 964 Bivins, A., North, D., Ahmad, A., Ahmed, W., Alm, E., Been, F., Bhattacharya, P., Bijlsma, L.,  
965 Boehm, A.B., Brown, J., Buttiglieri, G., Calabro, V., Carducci, A., Castiglioni, S.,  
966 Cetecioglu Gurol, Z., Chakraborty, S., Costa, F., Curcio, S., de los Reyes, F.L., Delgado  
967 Vela, J., Farkas, K., Fernandez-Casi, X., Gerba, C., Gerrity, D., Girones, R., Gonzalez,  
968 R., Haramoto, E., Harris, A., Holden, P.A., Islam, Md.T., Jones, D.L., Kasprzyk-Hordern,  
969 B., Kitajima, M., Kotlarz, N., Kumar, M., Kuroda, K., La Rosa, G., Malpei, F., Mautus, M.,  
970 McLellan, S.L., Medema, G., Meschke, J.S., Mueller, J., Newton, R.J., Nilsson, D.,  
971 Noble, R.T., van Nuijs, A., Peccia, J., Perkins, T.A., Pickering, A.J., Rose, J., Sanchez,  
972 G., Smith, A., Stadler, L., Stauber, C., Thomas, K., van der Voorn, T., Wigginton, K.,  
973 Zhu, K., Bibby, K., 2020. Wastewater-Based Epidemiology: Global Collaborative to  
974 Maximize Contributions in the Fight Against COVID-19. *Environ. Sci. Technol.* 54, 7754–  
975 7757. <https://doi.org/10.1021/acs.est.0c02388>
- 976 Cassidy, M., Fagone, J., 2020. 200 Chino inmates transferred to San Quentin, Corcoran. Why  
977 weren't they tested first? *San Franc. Chron.*

- 978 Catalogue of Bias Collaboration, Nunan, D., Bankhead, C., Aronson, J., 2017. Selection bias  
979 [WWW Document]. *Cat. Bias*. URL <https://catalogofbias.org/biases/selection-bias/>  
980 (accessed 4.22.21).
- 981 CDCR Population COVID-19 Tracking [WWW Document], n.d. [https://data.ca.gov/dataset/cdcr-](https://data.ca.gov/dataset/cdcr-population-covid-19-tracking)  
982 [population-covid-19-tracking](https://data.ca.gov/dataset/cdcr-population-covid-19-tracking) (accessed 4.15.21).
- 983 Chamie, G., Marquez, C., Crawford, E., Peng, J., Petersen, M., Schwab, D., Schwab, J.,  
984 Martinez, J., Jones, D., Black, D., Gandhi, M., Kerkhoff, A.D., Jain, V., Sergi, F., Jacobo,  
985 J., Rojas, S., Tulier-Laiwa, V., Gallardo-Brown, T., Appa, A., Chiu, C., Rodgers, M.,  
986 Hackett, J., Kistler, A., Hao, S., Kamm, J., Dynerman, D., Batson, J., Greenhouse, B.,  
987 DeRisi, J., Havlir, D.V., 2020. SARS-CoV-2 Community Transmission disproportionately  
988 affects Latinx population during Shelter-in-Place in San Francisco. *Clin. Infect. Dis. Off.*  
989 *Publ. Infect. Dis. Soc. Am.* <https://doi.org/10.1093/cid/ciaa1234>
- 990 Chen, C., Kostakis, C., Gerber, J.P., Tschärke, B.J., Irvine, R.J., White, J.M., 2014. Towards  
991 finding a population biomarker for wastewater epidemiology studies. *Sci. Total Environ.*  
992 487, 621–628. <https://doi.org/10.1016/j.scitotenv.2013.11.075>
- 993 Choi, P.M., Tschärke, B.J., Donner, E., O'Brien, J.W., Grant, S.C., Kaserzon, S.L., Mackie, R.,  
994 O'Malley, E., Crosbie, N.D., Thomas, K.V., Mueller, J.F., 2018. Wastewater-based  
995 epidemiology biomarkers: Past, present and future. *TrAC Trends Anal. Chem.* 105, 453–  
996 469. <https://doi.org/10.1016/j.trac.2018.06.004>
- 997 Coryell, M.P., Iakiviak, M., Pereira, N., Murugkar, P.P., Rippe, J., Williams, D.B., Hastie, J.L.,  
998 Sava, R.L., Lien, C.Z., Wang, T.T., Muller, W.J., Fischbach, M.A., Carlson, P.E., 2020.  
999 Validation and testing of a method for detection of SARS-CoV-2 RNA in healthy human  
1000 stool. *medRxiv*. <https://doi.org/10.1101/2020.11.09.20228601>
- 1001 Covid-WEB [WWW Document], n.d. Covid 19 Wastewater Epidemiology. Bay Area. URL  
1002 <https://www.covid-web.org> (accessed 4.12.21).
- 1003 D'Aoust, P.M., Graber, T.E., Mercier, E., Montpetit, D., Alexandrov, I., Neault, N., Baig, A.T.,  
1004 Mayne, J., Zhang, X., Alain, T., Servos, M.R., Srikanthan, N., MacKenzie, M., Figeys, D.,  
1005 Manuel, D., Jüni, P., MacKenzie, A.E., Delatolla, R., 2021a. Catching a resurgence:  
1006 Increase in SARS-CoV-2 viral RNA identified in wastewater 48 h before COVID-19  
1007 clinical tests and 96 h before hospitalizations. *Sci. Total Environ.* 770, 145319.  
1008 <https://doi.org/10.1016/j.scitotenv.2021.145319>
- 1009 D'Aoust, P.M., Mercier, E., Montpetit, D., Jia, J.-J., Alexandrov, I., Neault, N., Baig, A.T., Mayne,  
1010 J., Zhang, X., Alain, T., Langlois, M.-A., Servos, M.R., MacKenzie, M., Figeys, D.,  
1011 MacKenzie, A.E., Graber, T.E., Delatolla, R., 2021b. Quantitative analysis of SARS-  
1012 CoV-2 RNA from wastewater solids in communities with low COVID-19 incidence and  
1013 prevalence. *Water Res.* 188, 116560. <https://doi.org/10.1016/j.watres.2020.116560>
- 1014 Edwards, R.A., Vega, A.A., Norman, H.M., Ohaeri, M., Levi, K., Dinsdale, E.A., Cinek, O., Aziz,  
1015 R.K., McNair, K., Barr, J.J., Bibby, K., Brouns, S.J.J., Cazares, A., de Jonge, P.A.,  
1016 Desnues, C., Díaz Muñoz, S.L., Fineran, P.C., Kurilshikov, A., Lavigne, R., Mazankova,  
1017 K., McCarthy, D.T., Nobrega, F.L., Reyes Muñoz, A., Tapia, G., Trefault, N., Tyakht,  
1018 A.V., Vinuesa, P., Wagemans, J., Zhernakova, A., Aarestrup, F.M., Ahmadov, G.,  
1019 Alassaf, A., Anton, J., Asangba, A., Billings, E.K., Cantu, V.A., Carlton, J.M., Cazares,  
1020 D., Cho, G.-S., Condeff, T., Cortés, P., Cranfield, M., Cuevas, D.A., De la Iglesia, R.,  
1021 Decewicz, P., Doane, M.P., Dominy, N.J., Dziewit, L., Elwasila, B.M., Eren, A.M., Franz,  
1022 C., Fu, J., Garcia-Aljaro, C., Ghedin, E., Gulino, K.M., Haggerty, J.M., Head, S.R.,  
1023 Hendriksen, R.S., Hill, C., Hyöty, H., Ilina, E.N., Irwin, M.T., Jeffries, T.C., Jofre, J.,  
1024 Junge, R.E., Kelley, S.T., Khan Mirzaei, M., Kowalewski, M., Kumaresan, D., Leigh,  
1025 S.R., Lipson, D., Lisitsyna, E.S., Llagostera, M., Maritz, J.M., Marr, L.C., McCann, A.,  
1026 Molshanski-Mor, S., Monteiro, S., Moreira-Grez, B., Morris, M., Mugisha, L., Muniesa,  
1027 M., Neve, H., Nguyen, N., Nigro, O.D., Nilsson, A.S., O'Connell, T., Odeh, R., Oliver, A.,  
1028 Piuri, M., Prussin Ii, A.J., Qimron, U., Quan, Z.-X., Rainetova, P., Ramírez-Rojas, A.,

- 1029 Raya, R., Reasor, K., Rice, G.A.O., Rossi, A., Santos, R., Shimashita, J., Stachler, E.N.,  
1030 Stene, L.C., Strain, R., Stumpf, R., Torres, P.J., Twaddle, A., Ugochi Ibekwe, M.,  
1031 Villagra, N., Wandro, S., White, B., Whiteley, A., Whiteson, K.L., Wijmenga, C.,  
1032 Zambrano, M.M., Zschach, H., Dutilh, B.E., 2019. Global phylogeography and ancient  
1033 evolution of the widespread human gut virus crAssphage. *Nat. Microbiol.* 4, 1727–1736.  
1034 <https://doi.org/10.1038/s41564-019-0494-6>
- 1035 Feng, S., Roguet, A., McClary-Gutierrez, J.S., Newton, R.J., Kloczko, N., Meiman, J.G.,  
1036 McLellan, S.L., 2021. Evaluation of sampling frequency and normalization of SARS-  
1037 CoV-2 wastewater concentrations for capturing COVID-19 burdens in the community.  
1038 *medRxiv*. <https://doi.org/10.1101/2021.02.17.21251867>
- 1039 Gerrity, D., Papp, K., Stoker, M., Sims, A., Frehner, W., 2021. Early-pandemic wastewater  
1040 surveillance of SARS-CoV-2 in Southern Nevada: Methodology, occurrence, and  
1041 incidence/prevalence considerations. *Water Res.* X 10, 100086.  
1042 <https://doi.org/10.1016/j.wroa.2020.100086>
- 1043 Gibas, C., Lambirth, K., Mittal, N., Juel, M.A.I., Barua, V.B., Brazell, L.R., Hinton, K., Lontai, J.,  
1044 Stark, N., Young, I., Quach, C., Russ, M., Kauer, J., Nicolosi, B., Akella, S., Tang, W.,  
1045 Chen, D., Schlueter, J., Munir, M., 2021. Implementing Building-Level SARS-CoV-2  
1046 Wastewater Surveillance on a University Campus. *medRxiv*.  
1047 <https://doi.org/10.1101/2020.12.31.20248843>
- 1048 Gonzalez, R., Curtis, K., Bivins, A., Bibby, K., Weir, M.H., Yetka, K., Thompson, H., Keeling, D.,  
1049 Mitchell, J., Gonzalez, D., 2020. COVID-19 surveillance in Southeastern Virginia using  
1050 wastewater-based epidemiology. *Water Res.* 186, 116296.  
1051 <https://doi.org/10.1016/j.watres.2020.116296>
- 1052 Graham, K., Loeb, S., Wolfe, M., Catoe, D., Sinnott-Armstrong, N., Kim, S., Yamahara, K.,  
1053 Sassoubre, L., Mendoza, L., Roldan-Hernandez, L., Li, L., Wigginton, K., Boehm, A.,  
1054 2020. SARS-CoV-2 in wastewater settled solids is associated with COVID-19 cases in a  
1055 large urban sewershed. *medRxiv*. <https://doi.org/10.1101/2020.09.14.20194472>
- 1056 Green, H., Wilder, M., Collins, M., Fenty, A., Gentile, K., Kmush, B.L., Zeng, T., Middleton, F.A.,  
1057 Larsen, D.A., 2020. Quantification of SARS-CoV-2 and cross-assembly phage  
1058 (crAssphage) from wastewater to monitor coronavirus transmission within communities.  
1059 *medRxiv*. <https://doi.org/10.1101/2020.05.21.20109181>
- 1060 Greenwald, H., 2021. One-Step RT-qPCR for SARS-CoV-2 Wastewater Surveillance: N1,  
1061 PMMoV, BCoV, SOC, CrAssphage, Bacteroides rRNA, 18S rRNA.  
1062 <https://doi.org/10.17504/protocols.io.bsgvnbw6>
- 1063 Griffith, G.J., Morris, T.T., Tudball, M.J., Herbert, A., Mancano, G., Pike, L., Sharp, G.C., Sterne,  
1064 J., Palmer, T.M., Davey Smith, G., Tilling, K., Zuccolo, L., Davies, N.M., Hemani, G.,  
1065 2020. Collider bias undermines our understanding of COVID-19 disease risk and  
1066 severity. *Nat. Commun.* 11, 5749. <https://doi.org/10.1038/s41467-020-19478-2>
- 1067 Hart, O.E., Halden, R.U., 2020a. Modeling wastewater temperature and attenuation of sewage-  
1068 borne biomarkers globally. *Water Res.* 172, 115473.  
1069 <https://doi.org/10.1016/j.watres.2020.115473>
- 1070 Hart, O.E., Halden, R.U., 2020b. Computational analysis of SARS-CoV-2/COVID-19  
1071 surveillance by wastewater-based epidemiology locally and globally: Feasibility,  
1072 economy, opportunities and challenges. *Sci. Total Environ.* 730, 138875.  
1073 <https://doi.org/10.1016/j.scitotenv.2020.138875>
- 1074 Hata, A., Honda, R., 2020. Potential Sensitivity of Wastewater Monitoring for SARS-CoV-2:  
1075 Comparison with Norovirus Cases. *Environ. Sci. Technol.* 54, 6451–6452.  
1076 <https://doi.org/10.1021/acs.est.0c02271>
- 1077 Hoffmann, T., Alsing, J., 2021. Faecal shedding models for SARS-CoV-2 RNA amongst  
1078 hospitalised patients and implications for wastewater-based epidemiology. *medRxiv*.  
1079 <https://doi.org/10.1101/2021.03.16.21253603>



- 1080 Jacoby, W.G., 2000. Loess: a nonparametric, graphical tool for depicting relationships between  
1081 variables. *Elect. Stud.* 19, 577–613. [https://doi.org/10.1016/S0261-3794\(99\)00028-1](https://doi.org/10.1016/S0261-3794(99)00028-1)
- 1082 Kantor, R.S., Nelson, K.L., Greenwald, H.D., Kennedy, L.C., 2021. Challenges in Measuring the  
1083 Recovery of SARS-CoV-2 from Wastewater. *Environ. Sci. Technol.* 55, 3514–3519.  
1084 <https://doi.org/10.1021/acs.est.0c08210>
- 1085 Kapoor, V., Pitkänen, T., Ryu, H., Elk, M., Wendell, D., Domingo, J.W.S., 2015. Distribution of  
1086 Human-Specific Bacteroidales and Fecal Indicator Bacteria in an Urban Watershed  
1087 Impacted by Sewage Pollution, Determined Using RNA- and DNA-Based Quantitative  
1088 PCR Assays. *Appl. Environ. Microbiol.* 81, 91–99. <https://doi.org/10.1128/AEM.02446-14>
- 1089 Kyurkchiev, N., Markov, S., 2016. On the Hausdorff distance between the Heaviside step  
1090 function and Verhulst logistic function. *J. Math. Chem.* 54, 109–119.  
1091 <https://doi.org/10.1007/s10910-015-0552-0>
- 1092 Li, L., Tan, C., Zeng, J., Luo, C., Hu, S., Peng, Y., Li, W., Xie, Z., Ling, Y., Zhang, X., Deng, E.,  
1093 Xu, H., Wang, J., Xie, Y., Zhou, Y., Zhang, W., Guo, Y., Liu, Z., 2021. Analysis of viral  
1094 load in different specimen types and serum antibody levels of COVID-19 patients. *J.*  
1095 *Transl. Med.* 19, 30. <https://doi.org/10.1186/s12967-020-02693-2>
- 1096 McClary-Gutierrez, J., Mattioli, M., Marcenac, P., Silverman, A., Boehm, A., Bibby, K., Balliet,  
1097 M., Iij, F. de los R., Gerrity, D., Griffith, J., Holden, P., Katehis, D., Kester, G., LaCross,  
1098 N., Lipp, E., Meiman, J., Noble, R., Brossard, D., McLellan, S., 2021. Sars-Cov-2  
1099 Wastewater Surveillance for Public Health Action: Connecting Perspectives From  
1100 Wastewater Researchers and Public Health Officials During a Global Pandemic.  
1101 <https://doi.org/10.20944/preprints202104.0167.v1>
- 1102 McLellan, S.L., Feng, S., Roguet, A., McClary-Gutierrez, J.S., Newton, R.J., Kloczko, N.,  
1103 Meiman, J.G., 2021. Evaluation of sampling frequency and normalization of SARS-CoV-  
1104 2 wastewater concentrations for capturing COVID-19 burdens in the community.  
1105 medRxiv. <https://doi.org/10.1101/2021.02.17.21251867>
- 1106 Medema, G., Heijnen, L., Elsinga, G., Italiaander, R., Brouwer, A., 2020. Presence of SARS-  
1107 Coronavirus-2 RNA in Sewage and Correlation with Reported COVID-19 Prevalence in  
1108 the Early Stage of the Epidemic in The Netherlands. *Environ. Sci. Technol. Lett.* 7, 511–  
1109 516. <https://doi.org/10.1021/acs.estlett.0c00357>
- 1110 Misa, N.-Y., Perez, B., Basham, K., Fisher-Hobson, E., Butler, B., King, K., White, D.A.E.,  
1111 Anderson, E.S., 2020. Racial/ethnic disparities in COVID-19 disease burden & mortality  
1112 among emergency department patients in a safety net health system. *Am. J. Emerg.*  
1113 *Med.* <https://doi.org/10.1016/j.ajem.2020.09.053>
- 1114 Montoya-Barthelemy, A.G., Lee, C.D., Cundiff, D.R., Smith, E.B., 2020. COVID-19 and the  
1115 Correctional Environment: The American Prison as a Focal Point for Public Health. *Am.*  
1116 *J. Prev. Med.* 58, 888–891. <https://doi.org/10.1016/j.amepre.2020.04.001>
- 1117 Murakami, M., Hata, A., Honda, R., Watanabe, T., 2020. Letter to the Editor: Wastewater-Based  
1118 Epidemiology Can Overcome Representativeness and Stigma Issues Related to COVID-  
1119 19. *Environ. Sci. Technol.* <https://doi.org/10.1021/acs.est.0c02172>
- 1120 Nemudryi, A., Nemudraia, A., Wiegand, T., Surya, K., Buyukyoruk, M., Cicha, C., Vanderwood,  
1121 K.K., Wilkinson, R., Wiedenheft, B., 2020. Temporal Detection and Phylogenetic  
1122 Assessment of SARS-CoV-2 in Municipal Wastewater. *Cell Rep. Med.* 1, 100098.  
1123 <https://doi.org/10.1016/j.xcrm.2020.100098>
- 1124 Nolan, T., Hands, R.E., Ogunkolade, W., Bustin, S.A., 2006. SPUD: A quantitative PCR assay  
1125 for the detection of inhibitors in nucleic acid preparations. *Anal. Biochem.* 351, 308–310.  
1126 <https://doi.org/10.1016/j.ab.2006.01.051>
- 1127 Parasa, S., Desai, M., Thoguluva Chandrasekar, V., Patel, H.K., Kennedy, K.F., Roesch, T.,  
1128 Spadaccini, M., Colombo, M., Gabbiadini, R., Artifon, E.L.A., Repici, A., Sharma, P.,  
1129 2020. Prevalence of Gastrointestinal Symptoms and Fecal Viral Shedding in Patients  
1130 With Coronavirus Disease 2019: A Systematic Review and Meta-analysis. *JAMA Netw.*

- 1131 Open 3, e2011335. <https://doi.org/10.1001/jamanetworkopen.2020.11335>
- 1132 Peccia, J., Zulli, A., Brackney, D.E., Grubaugh, N.D., Kaplan, E.H., Casanovas-Massana, A.,  
1133 Ko, A.I., Malik, A.A., Wang, D., Wang, M., Warren, J.L., Weinberger, D.M., Arnold, W.,  
1134 Omer, S.B., 2020. Measurement of SARS-CoV-2 RNA in wastewater tracks community  
1135 infection dynamics. *Nat. Biotechnol.* 38, 1164–1167. [https://doi.org/10.1038/s41587-020-](https://doi.org/10.1038/s41587-020-0684-z)  
1136 0684-z
- 1137 Pitkänen, T., Ryu, H., Elk, M., Hokajärvi, A.-M., Siponen, S., Vepsäläinen, A., Räsänen, P.,  
1138 Santo Domingo, J.W., 2013. Detection of Fecal Bacteria and Source Tracking Identifiers  
1139 in Environmental Waters Using rRNA-Based RT-qPCR and rDNA-Based qPCR Assays.  
1140 *Environ. Sci. Technol.* 47, 13611–13620. <https://doi.org/10.1021/es403489b>
- 1141 Polo, D., Quintela-Baluja, M., Corbishley, A., Jones, D.L., Singer, A.C., Graham, D.W.,  
1142 Romalde, J.L., 2020. Making waves: Wastewater-based epidemiology for COVID-19 –  
1143 approaches and challenges for surveillance and prediction. *Water Res.* 186, 116404.  
1144 <https://doi.org/10.1016/j.watres.2020.116404>
- 1145 Randazzo, W., Cuevas-Ferrando, E., Sanjuán, R., Domingo-Calap, P., Sánchez, G., 2020a.  
1146 Metropolitan wastewater analysis for COVID-19 epidemiological surveillance. *Int. J. Hyg.*  
1147 *Environ. Health* 230, 113621. <https://doi.org/10.1016/j.ijheh.2020.113621>
- 1148 Randazzo, W., Truchado, P., Cuevas-Ferrando, E., Simón, P., Allende, A., Sánchez, G., 2020b.  
1149 SARS-CoV-2 RNA in wastewater anticipated COVID-19 occurrence in a low prevalence  
1150 area. *Water Res.* 181, 115942. <https://doi.org/10.1016/j.watres.2020.115942>
- 1151 Schrader, C., Schielke, A., Ellerbroek, L., John, R., 2012. PCR inhibitors – occurrence,  
1152 properties and removal. *J. Appl. Microbiol.* 113, 1014–1026.  
1153 <https://doi.org/10.1111/j.1365-2672.2012.05384.x>
- 1154 Shanks, O.C., Atikovic, E., Blackwood, A.D., Lu, J., Noble, R.T., Domingo, J.S., Seifring, S.,  
1155 Sivaganesan, M., Haugland, R.A., 2008. Quantitative PCR for Detection and  
1156 Enumeration of Genetic Markers of Bovine Fecal Pollution. *Appl. Environ. Microbiol.* 74,  
1157 745–752. <https://doi.org/10.1128/AEM.01843-07>
- 1158 Sims, N., Kasprzyk-Hordern, B., 2020. Future perspectives of wastewater-based epidemiology:  
1159 Monitoring infectious disease spread and resistance to the community level. *Environ. Int.*  
1160 139, 105689. <https://doi.org/10.1016/j.envint.2020.105689>
- 1161 Source code for spatialEco package [WWW Document], n.d.  
1162 <https://rdrr.io/cran/spatialEco/src/R/poly.regression.R> (accessed 4.12.21).
- 1163 Source code for statsmodels module [WWW Document], n.d.  
1164 [https://www.statsmodels.org/dev/\\_modules/statsmodels/nonparametric/smoothers\\_lowess.html#lowess](https://www.statsmodels.org/dev/_modules/statsmodels/nonparametric/smoothers_lowess.html#lowess) (accessed 4.12.21).
- 1166 Stachler, E., Kelty, C., Sivaganesan, M., Li, X., Bibby, K., Shanks, O.C., 2017. Quantitative  
1167 CrAssphage PCR Assays for Human Fecal Pollution Measurement. *Environ. Sci.*  
1168 *Technol.* 51, 9146–9154. <https://doi.org/10.1021/acs.est.7b02703>
- 1169 Stadler, L.B., Ensor, K.B., Clark, J.R., Kalvapalle, P., LaTurner, Z.W., Mojica, L., Terwilliger, A.,  
1170 Zhuo, Y., Ali, P., Avadhanula, V., Bertolusso, R., Crosby, T., Hernandez, H., Hollstein,  
1171 M., Weesner, K., Zong, D.M., Persse, D., Piedra, P.A., Maresso, A.W., Hopkins, L.,  
1172 2020. Wastewater Analysis of SARS-CoV-2 as a Predictive Metric of Positivity Rate for a  
1173 Major Metropolis. *medRxiv*. <https://doi.org/10.1101/2020.11.04.20226191>
- 1174 Staley, C., Gordon, K.V., Schoen, M.E., Harwood, V.J., 2012. Performance of Two Quantitative  
1175 PCR Methods for Microbial Source Tracking of Human Sewage and Implications for  
1176 Microbial Risk Assessment in Recreational Waters. *Appl. Environ. Microbiol.* 78, 7317–  
1177 7326. <https://doi.org/10.1128/AEM.01430-12>
- 1178 Symonds, E.M., Rosario, K., Breitbart, M., 2019. Pepper mild mottle virus: Agricultural menace  
1179 turned effective tool for microbial water quality monitoring and assessing (waste)water  
1180 treatment technologies. *PLoS Pathog.* 15. <https://doi.org/10.1371/journal.ppat.1007639>
- 1181 Track Testing Trends [WWW Document], n.d. . Johns Hopkins Coronavirus Resource Center.

- 1182 <https://coronavirus.jhu.edu/testing/tracker> (accessed 4.12.21).
- 1183 Vallejo, J.A., Rumbo-Feal, S., Conde-Pérez, K., López-Oriona, Á., Tarrío, J., Reif, R., Ladra, S.,  
1184 Rodiño-Janeiro, B.K., Nasser, M., Cid, Á., Veiga, M.C., Acevedo, A., Lamora, C., Bou,  
1185 G., Cao, R., Poza, M., 2020. Highly predictive regression model of active cases of  
1186 COVID-19 in a population by screening wastewater viral load. medRxiv.  
1187 <https://doi.org/10.1101/2020.07.02.20144865>
- 1188 Walsh, K.A., Jordan, K., Clyne, B., Rohde, D., Drummond, L., Byrne, P., Ahern, S., Carty, P.G.,  
1189 O'Brien, K.K., O'Murchu, E., O'Neill, M., Smith, S.M., Ryan, M., Harrington, P., 2020.  
1190 SARS-CoV-2 detection, viral load and infectivity over the course of an infection. *J. Infect.*  
1191 81, 357–371. <https://doi.org/10.1016/j.jinf.2020.06.067>
- 1192 Whitney, O., 2020. V.4 - Direct wastewater RNA capture and purification via the Sewage, Salt,  
1193 Silica and SARS-CoV-2 (4S) method. <https://doi.org/10.17504/protocols.io.bpdfmi3n>
- 1194 Whitney, O.N., Kennedy, L.C., Fan, V.B., Hinkle, A., Kantor, R., Greenwald, H., Crits-Christoph,  
1195 A., Al-Shayeb, B., Chaplin, M., Maurer, A.C., Tjian, R., Nelson, K.L., 2021. Sewage, Salt,  
1196 Silica, and SARS-CoV-2 (4S): An Economical Kit-Free Method for Direct Capture of  
1197 SARS-CoV-2 RNA from Wastewater. *Environ. Sci. Technol.*  
1198 <https://doi.org/10.1021/acs.est.0c08129>
- 1199 Wilder, M.L., Middleton, F., Larsen, D.A., Du, Q., Fenty, A., Zeng, T., Insaf, T., Kilaru, P.,  
1200 Collins, M., Kmush, B., Green, H.C., 2021. Co-quantification of crAssphage increases  
1201 confidence in wastewater-based epidemiology for SARS-CoV-2 in low prevalence areas.  
1202 *Water Res. X* 100100. <https://doi.org/10.1016/j.wroa.2021.100100>
- 1203 Wood, M.D., Beresford, N.A., Copplestone, D., 2011. Limit of detection values in data analysis:  
1204 Do they matter? *Radioprotection* 46, S85–S90.  
1205 <https://doi.org/10.1051/radiopro/20116728s>
- 1206 Wu, F., Xiao, A., Zhang, J., Moniz, K., Endo, N., Armas, F., Bushman, M., Chai, P.R., Duvallet,  
1207 C., Erickson, T.B., Foppe, K., Ghaeli, N., Gu, X., Hanage, W.P., Huang, K.H., Lee, W.L.,  
1208 Matus, M., McElroy, K.A., Rhode, S.F., Wuertz, S., Thompson, J., Alm, E.J., 2021.  
1209 Wastewater Surveillance of SARS-CoV-2 across 40 U.S. states. medRxiv.  
1210 <https://doi.org/10.1101/2021.03.10.21253235>
- 1211 Wu, F., Zhang, J., Xiao, A., Gu, X., Lee, W.L., Armas, F., Kauffman, K., Hanage, W., Matus, M.,  
1212 Ghaeli, N., Endo, N., Duvallet, C., Poyet, M., Moniz, K., Washburne, A.D., Erickson,  
1213 T.B., Chai, P.R., Thompson, J., Alm, E.J., 2020. SARS-CoV-2 Titers in Wastewater Are  
1214 Higher than Expected from Clinically Confirmed Cases. *mSystems* 5.  
1215 <https://doi.org/10.1128/mSystems.00614-20>
- 1216 Wurtzer, S., Waldman, P., Ferrier-Rembert, A., Frenois-Veyrat, G., Mouchel, J., Boni, M.,  
1217 Maday, Y., Consortium, O., Marechal, V., Moulin, L., 2020. Several forms of SARS-CoV-  
1218 2 RNA can be detected in wastewaters : implication for wastewater-based epidemiology  
1219 and risk assessment. medRxiv. <https://doi.org/10.1101/2020.12.19.20248508>
- 1220 Xagorarakis, I., O'Brien, E., 2020. Wastewater-Based Epidemiology for Early Detection of Viral  
1221 Outbreaks, in: O'Bannon, D.J. (Ed.), *Women in Water Quality: Investigations by*  
1222 *Prominent Female Engineers, Women in Engineering and Science*. Springer  
1223 International Publishing, Cham, pp. 75–97. [https://doi.org/10.1007/978-3-030-17819-2\\_5](https://doi.org/10.1007/978-3-030-17819-2_5)
- 1224 Ye, Y., Ellenberg, R.M., Graham, K.E., Wigginton, K.R., 2016. Survivability, Partitioning, and  
1225 Recovery of Enveloped Viruses in Untreated Municipal Wastewater. *Environ. Sci.*  
1226 *Technol.* 50, 5077–5085. <https://doi.org/10.1021/acs.est.6b00876>
- 1227 Zahedi, A., Monis, P., Deere, D., Ryan, U., 2021. Wastewater-based epidemiology—  
1228 surveillance and early detection of waterborne pathogens with a focus on SARS-CoV-2,  
1229 *Cryptosporidium* and *Giardia*. *Parasitol. Res.* [https://doi.org/10.1007/s00436-020-07023-](https://doi.org/10.1007/s00436-020-07023-5)  
1230 5
- 1231 Zuccato, E., Chiabrando, C., Castiglioni, S., Calamari, D., Bagnati, R., Schiarea, S., Fanelli, R.,  
1232 2005. Cocaine in surface waters: a new evidence-based tool to monitor community drug

- 1233 abuse. Environ. Health 4, 14. <https://doi.org/10.1186/1476-069X-4-14>
- 1234 Zuccato Ettore, Chiabrando Chiara, Castiglioni Sara, Bagnati Renzo, Fanelli Roberto, 2008.
- 1235 Estimating Community Drug Abuse by Wastewater Analysis. Environ. Health Perspect.
- 1236 116, 1027–1032. <https://doi.org/10.1289/ehp.11022>